Some reference simulations from laboratory to planetary scale

By Nils Wedi with many thanks to Piotr Smolarkiewicz!

Outline

- **Examples with time-dependent lower and upper boundaries**
- **Energy budget for wave-driven flows**
- **Time-dependent lateral meridional boundaries**
- **Local- and global-scale simulations on the reduced-radius sphere**

Time-dependent curvilinear boundaries

- **Exploit a metric structure determined by data …**
  Prusa, Smolarkiewicz and Garcia (1996); Prusa and Smolarkiewicz (2003); Wedi and Smolarkiewicz (2004)

$$\overline{x}^1 \equiv \overline{x} = E(x,y,t)$$
$$\overline{x}^2 \equiv \overline{y} = D(x,y,t)$$
$$\overline{x}^3 \equiv \overline{z} = C(x,y,z,t) = C(\xi)$$

$$\xi = \xi(x,y,z,t) := H_0 \frac{z - z_s(x,y,t)}{H(x,y,t) - z_s(x,y,t)}$$

```
compute coordinate transformation related matrices
      call topolog(x,y)             # define zs, zh
c     call shallow(it,rho,x,y)      # alternative zh
      call metryc(x,y,z)            # define coordinates

compute base state, environmental, and absorber profiles
      call tinit(z,x,y,tau,lipps,initi)

create boundary values for velocity
      call velbc(ue,ve,rho)
```

Metric coefficients

$$\rho^* := \rho_b \overline{G},$$

$$\widetilde{G}^k_j := \sqrt{g^{jj}}(\partial \overline{x}^k / \partial x^j),$$

$$\overline{v^*}^k := d\overline{x}^k / d\overline{t} := \dot{\overline{x}}^k \; ,$$

$$\overline{v^s}^k := \overline{v^*}^k - \frac{\partial \overline{x}^k}{\partial t},$$

$$\overline{v^s}^k = \widetilde{G}^n_j v^n$$

```
g110=1./((1-icylind)*gmm(i,j,k)*cosa(i,j)+icylind*1.)
g220=1./gmm(i,j,k)
g11=strxx(i,j)*g110
g12=stryx(i,j)*g110
g13=(s13(i,j)*gmul(k)-h13(i,j))*gmus(k)*g110
g21=strxy(i,j)*g220
g22=stryy(i,j)*g220
g23=(s23(i,j)*gmul(k)-h23(i,j))*gmus(k)*g220
g33=gi(i,j)*gmus(k)
ox(i,j,k,0)=g11*u(i,j,k,0)+g21*v(i,j,k,0)
oy(i,j,k,0)=g12*u(i,j,k,0)+g22*v(i,j,k,0)
oz(i,j,k,0)=g13*u(i,j,k,0)+g23*v(i,j,k,0)+g33*w(i,j,k,0)
```

Generalized coordinate equations in potential temperature

$$\frac{\partial(\rho^* \overline{v^s}^k)}{\partial \overline{x}^k} = 0 \ ,$$

$$\frac{dv^j}{d\overline{t}} = - \ \widetilde{G}_j^k \frac{\partial \pi'}{\partial \overline{x}^k} + g \frac{\theta'}{\theta_b} \delta_3{}^j + F^j \ ,$$

$$\frac{d\theta'}{d\overline{t}} = -\overline{v^s}^k \frac{\partial \theta_e}{\partial \overline{x}^k}$$

```
! Anelastic in theta (lipps=1,2,3)
     th0(i,j,k)
! Boussinesq (lipps=0)
!    th0(i,j,k) = th00
     Gmod =dth*g/th0(i,j,k)*astri
     Gmodt=dth*g/th0(i,j,k)*astrti
     . . . Gmodt*th(i,j,k) . . .
```


ECMWF

Gravity waves

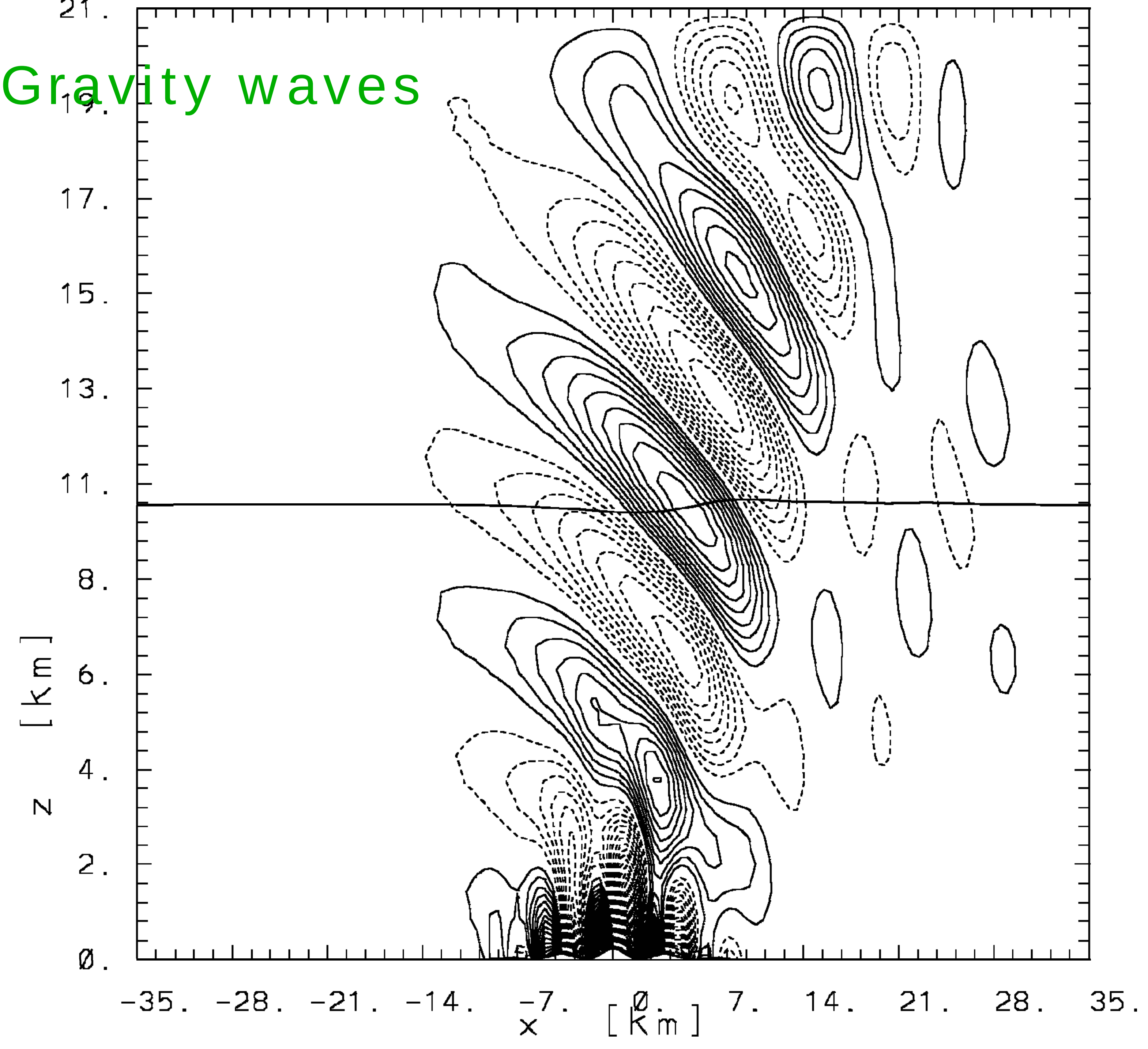

Reduced domain simulation

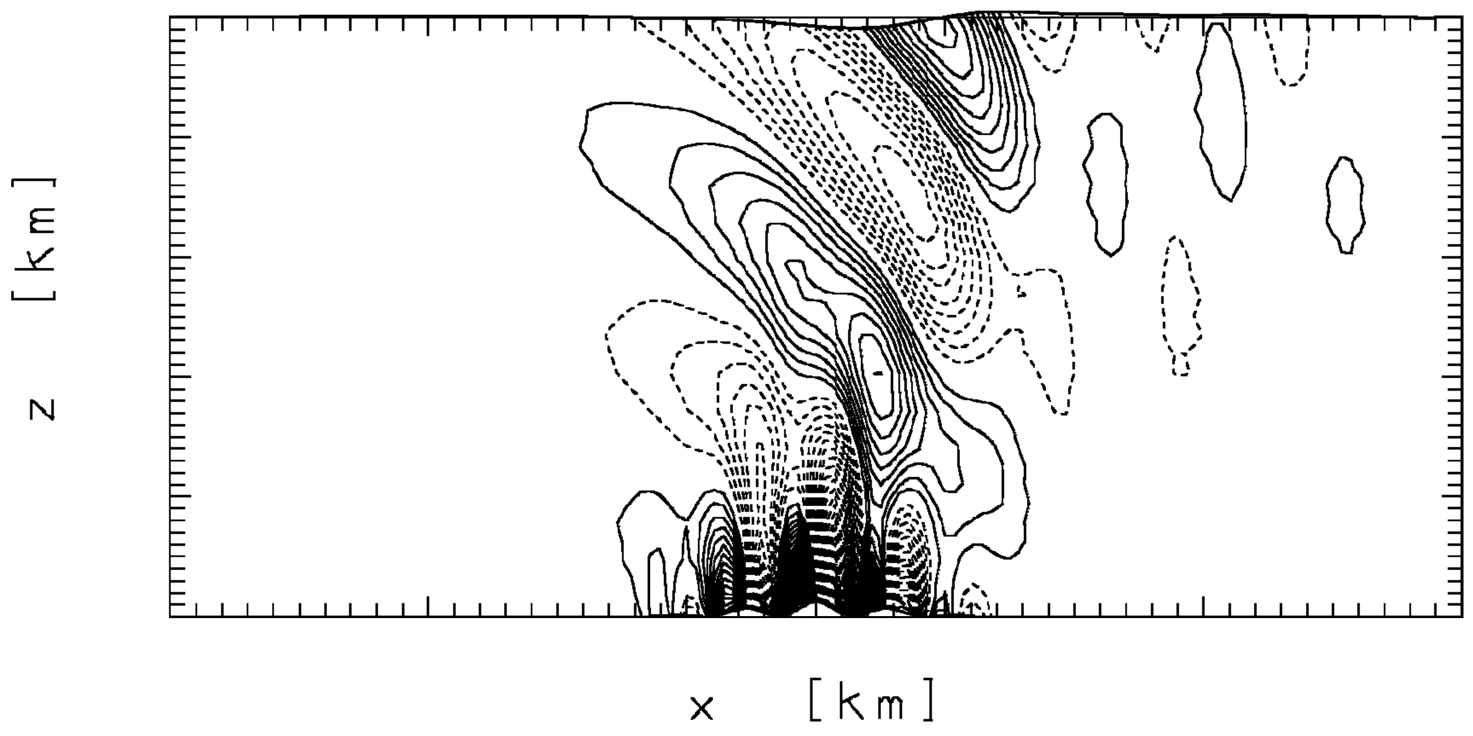

Another practical example

- **Incorporate an approximate free-surface boundary into non-hydrostatic ocean models**
- **“Single layer” simulation with an auxiliary boundary model given by the solution of the shallow water equations**
- **Comparison to a “two-layer” simulation with density discontinuity 1/1000**

- **collapses the relationship between auxiliary boundary models and the interior fluid domain to a single variable and it’s derivative!**
- **does not provide a direct way to predict *zh* itself, but it facilitates the coupling to data, other algorithms or parametrizations that do.**

Incompressible Euler Equations

```
!incompress Euler: th,the density!
! Set th00=rh00=1
rhoinc=th(i,j,k)+the(i,j,k)
Gmod =-dth*g/rhoinc*astri
Gmodt=-dth*g/rhoinc*astrti
     . . . Gmodt*th(i,j,k) . . .
```

$$\frac{\partial(\overline{G}\overline{v^s}^k)}{\partial\overline{x}^k} = 0 \,,$$

$$\frac{dv^j}{d\bar{t}} = -\frac{1}{\rho}\,\widetilde{G}_j^k \frac{\partial\phi'}{\partial\overline{x}^k} - g\left(1 - \frac{\rho_e}{\rho}\right)\delta_3{}^j$$

$$\frac{d\rho}{d\bar{t}} = 0$$

Use semi-Lagrangian option!

Incompressible Euler Equations

$$\Rightarrow \quad -\frac{\Delta t}{\rho^*}\sum_{i=1}^{3}\frac{\partial}{\partial \overline{x}^i}\left[\rho^*\mathcal{E}^{-1}\left(\mathcal{V}^i-\sum_{j=1}^{3}C^{ij}\frac{\partial \pi'}{\partial \overline{x}^j}\right)\right]=0$$

instead …

1/ρ should have been added here …

```
c incompress Euler
ox(i,j,k,1)=ox(i,j,k,1)*rhoinc
oy(i,j,k,1)=oy(i,j,k,1)*rhoinc
oz(i,j,k,1)=oz(i,j,k,1)*rhoinc

etainv=( -Gmod*dthe(i,j,k,1)*F2str
.            +Gmod*dthe(i,j,k,2)*F2str*F3str
.            +Gmod*dthe(i,j,k,3)*(1.+F3str*F3str)
.            +Rt*(1.+F2str*F2str+F3str*F3str) )*(1.+astr)
c incompress Euler
.           *rhoinc
295 continue
```

Regime diagram

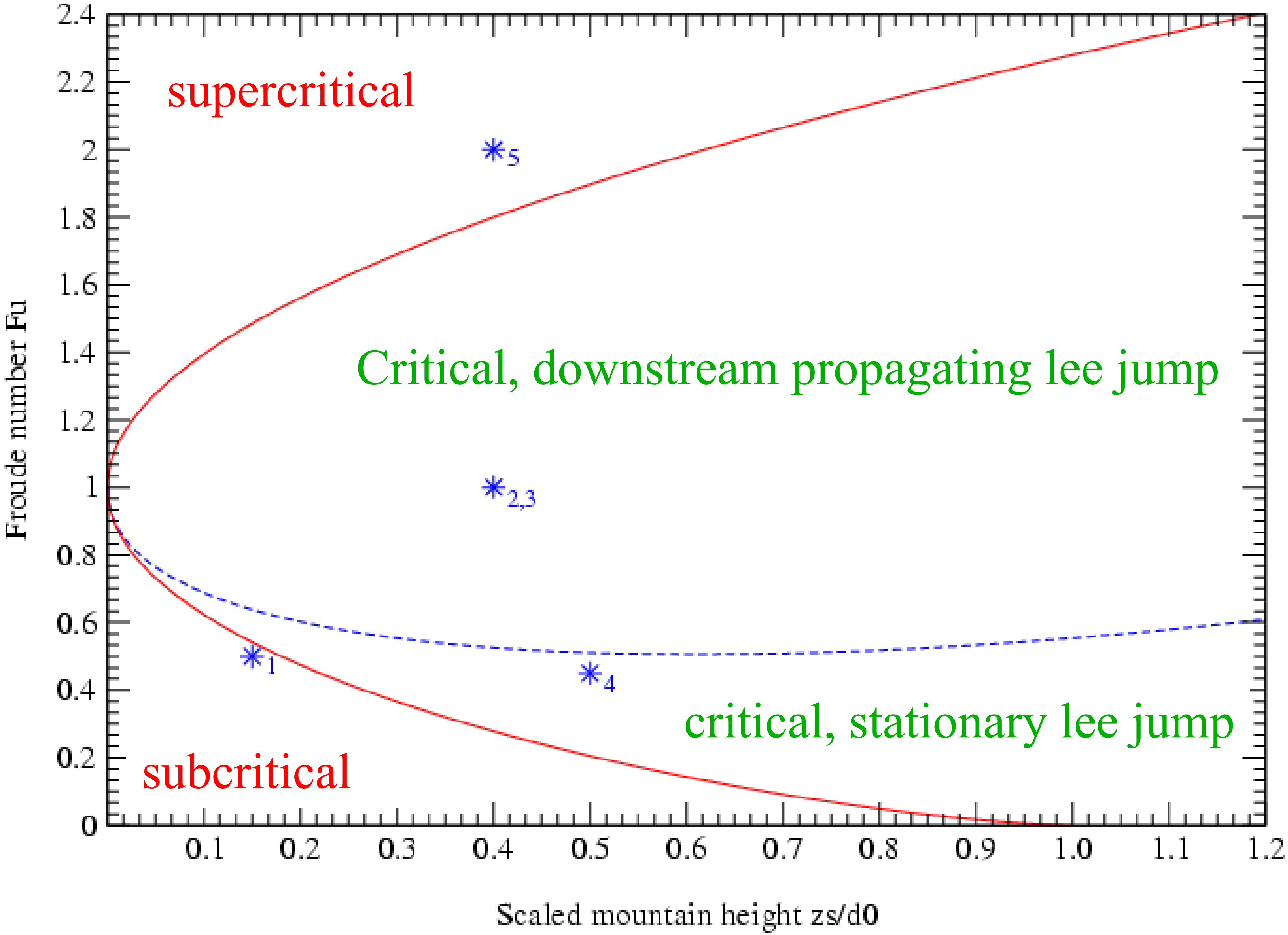

ECMWF

Critical – “two-layer”

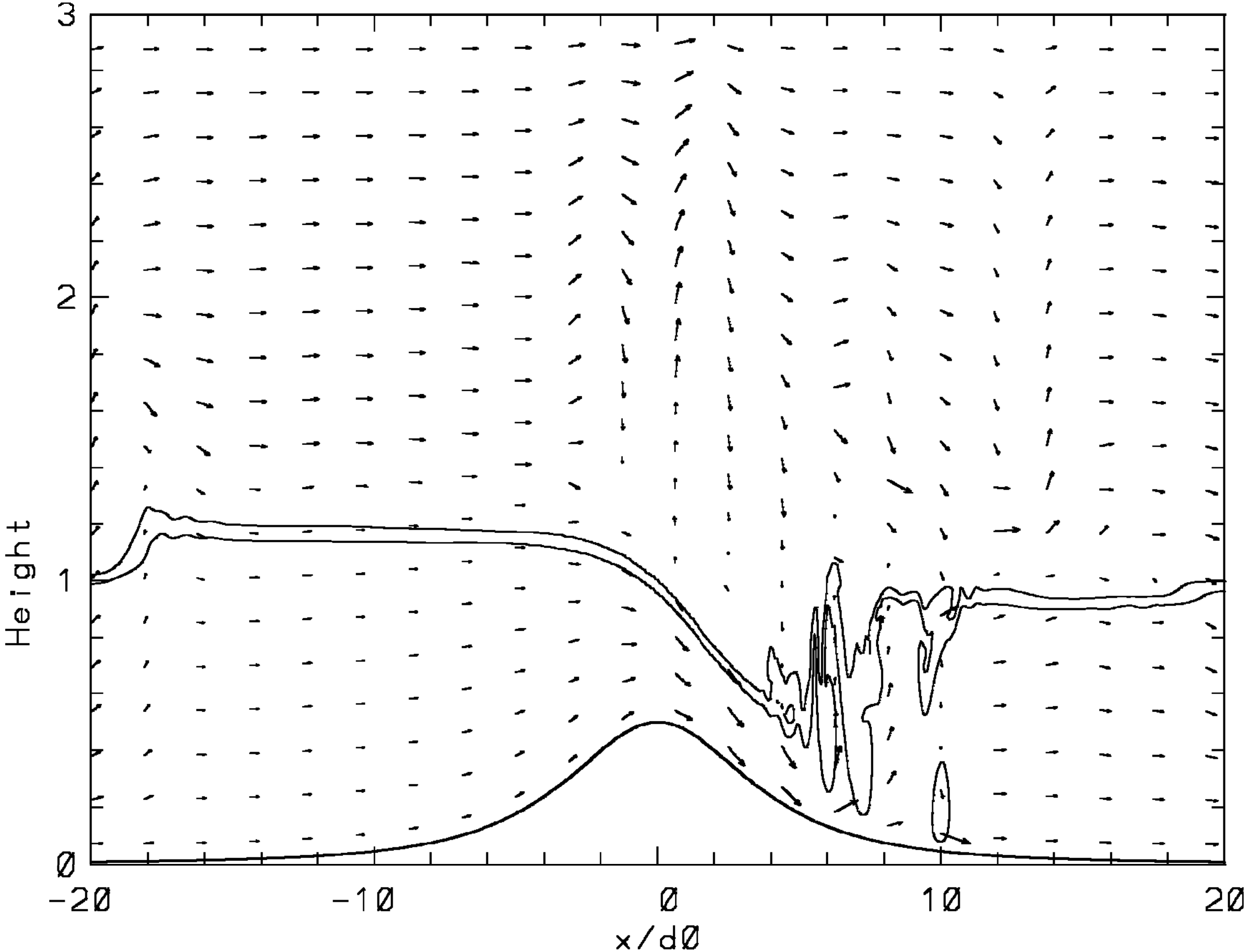

ECMWF

Critical – reduced domain

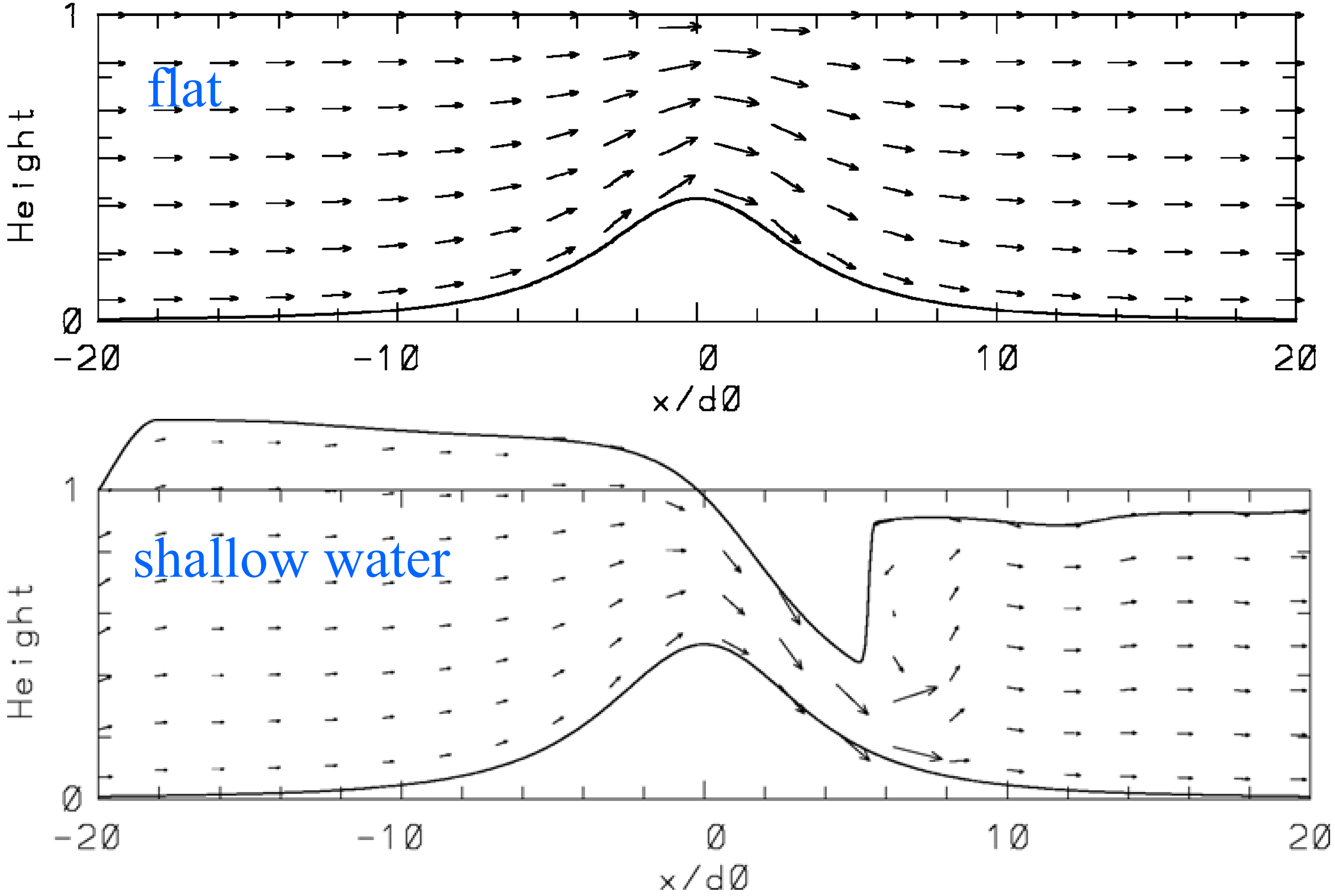

Critical, downstream propagating lee jump

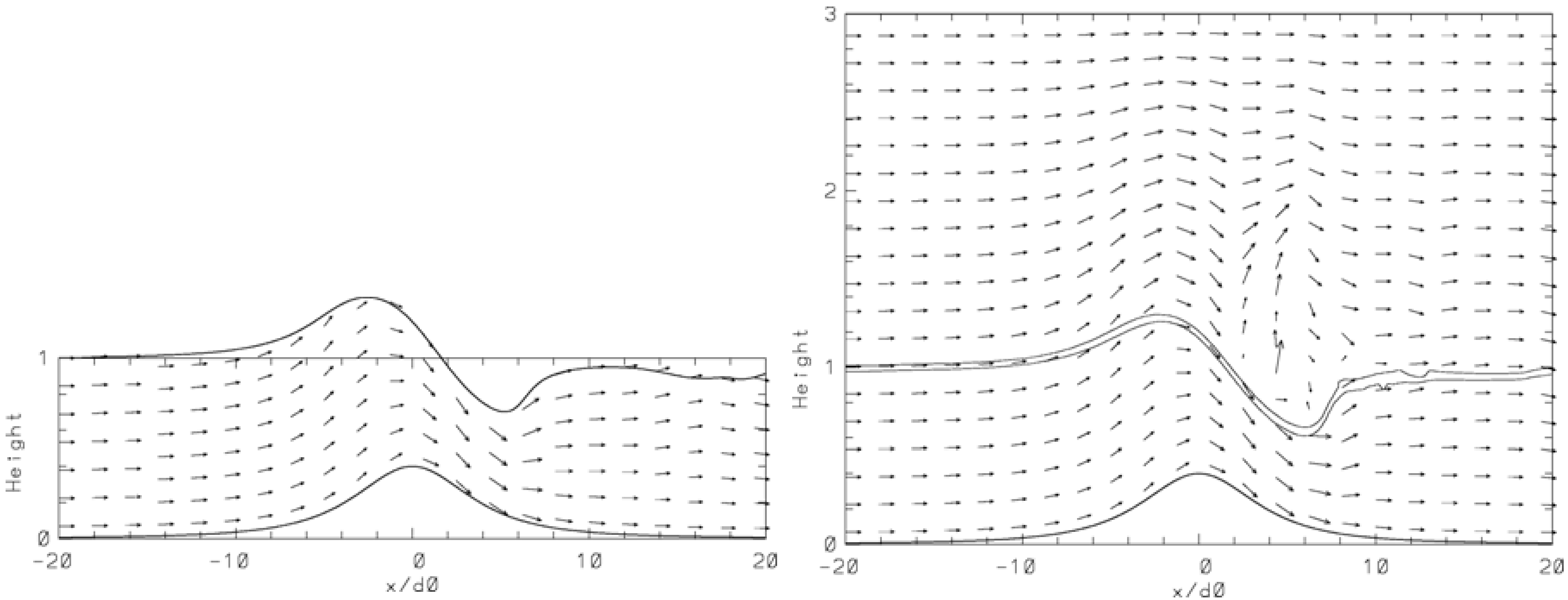

ECMWF

Critical, downstream propagating lee jump

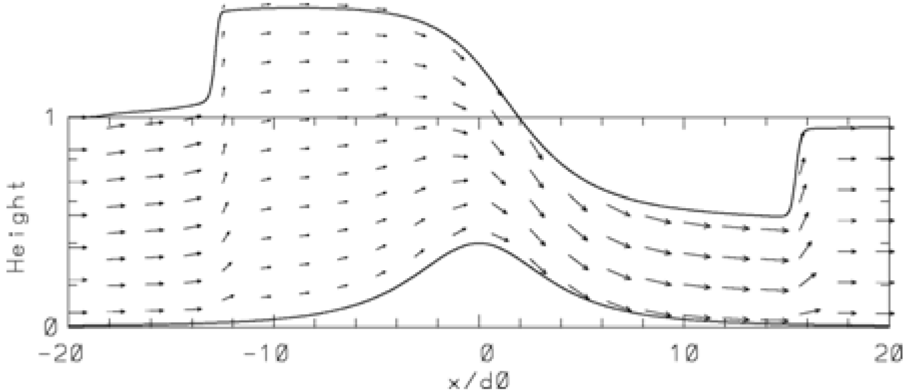

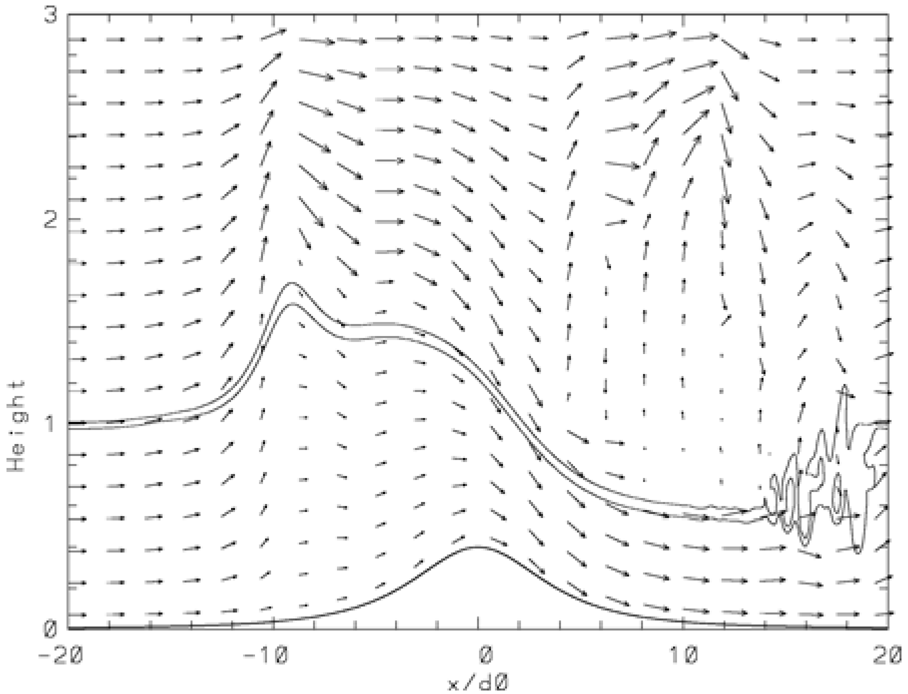

ECMWF

The stratospheric QBO

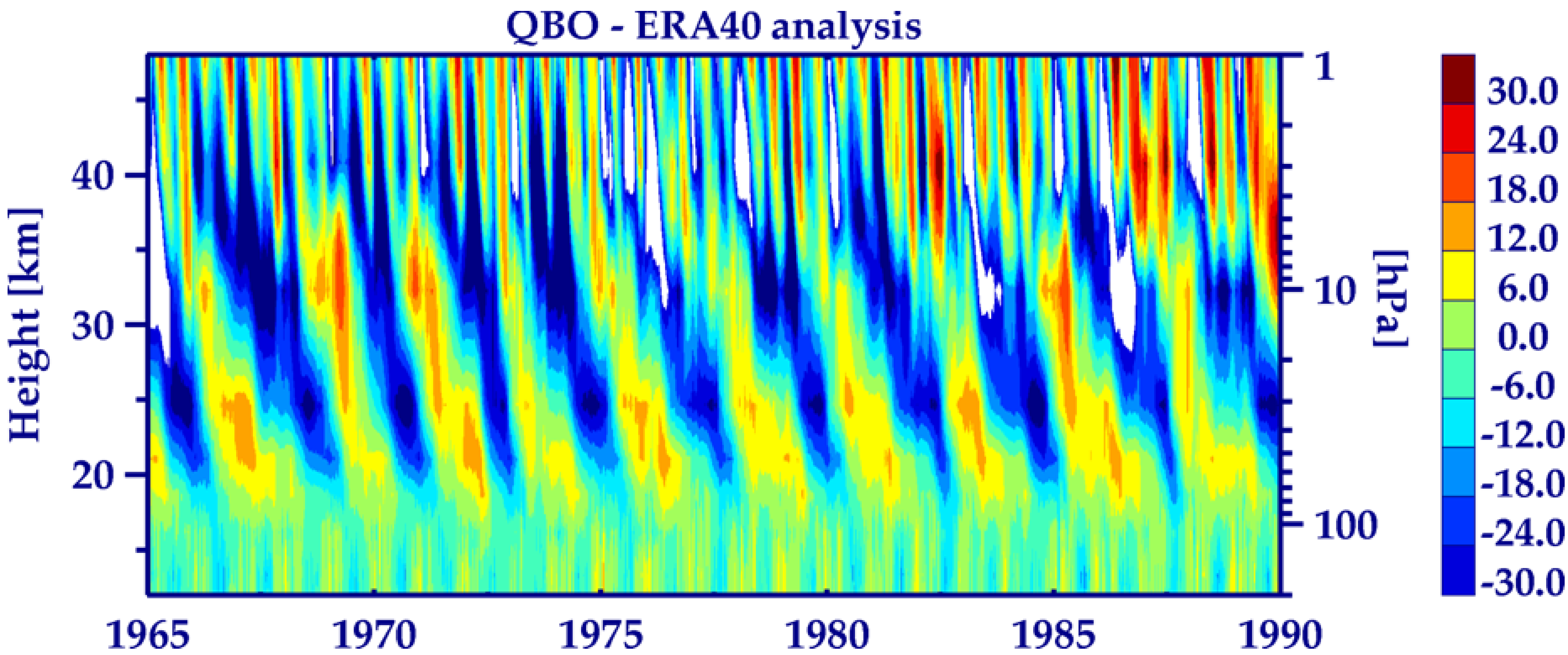

- westward

+ eastward

(unfiltered) ERA40 data *(Uppala et al, 2005)*

ECMWF

The laboratory experiment of Plumb and McEwan

- **The principal mechanism of the QBO was demonstrated in the laboratory** *Plumb and McEwan, J. Atmos. Sci. 35 1827-1839 (1978)*
- **University of Kyoto**
  http://www.gfd-dennou.org/library/gfd_exp/exp_e/index.htm

Animation:

(Wedi and Smolarkiewicz, J. Atmos. Sci., 2006)

Schematic description of the QBO laboratory analogue

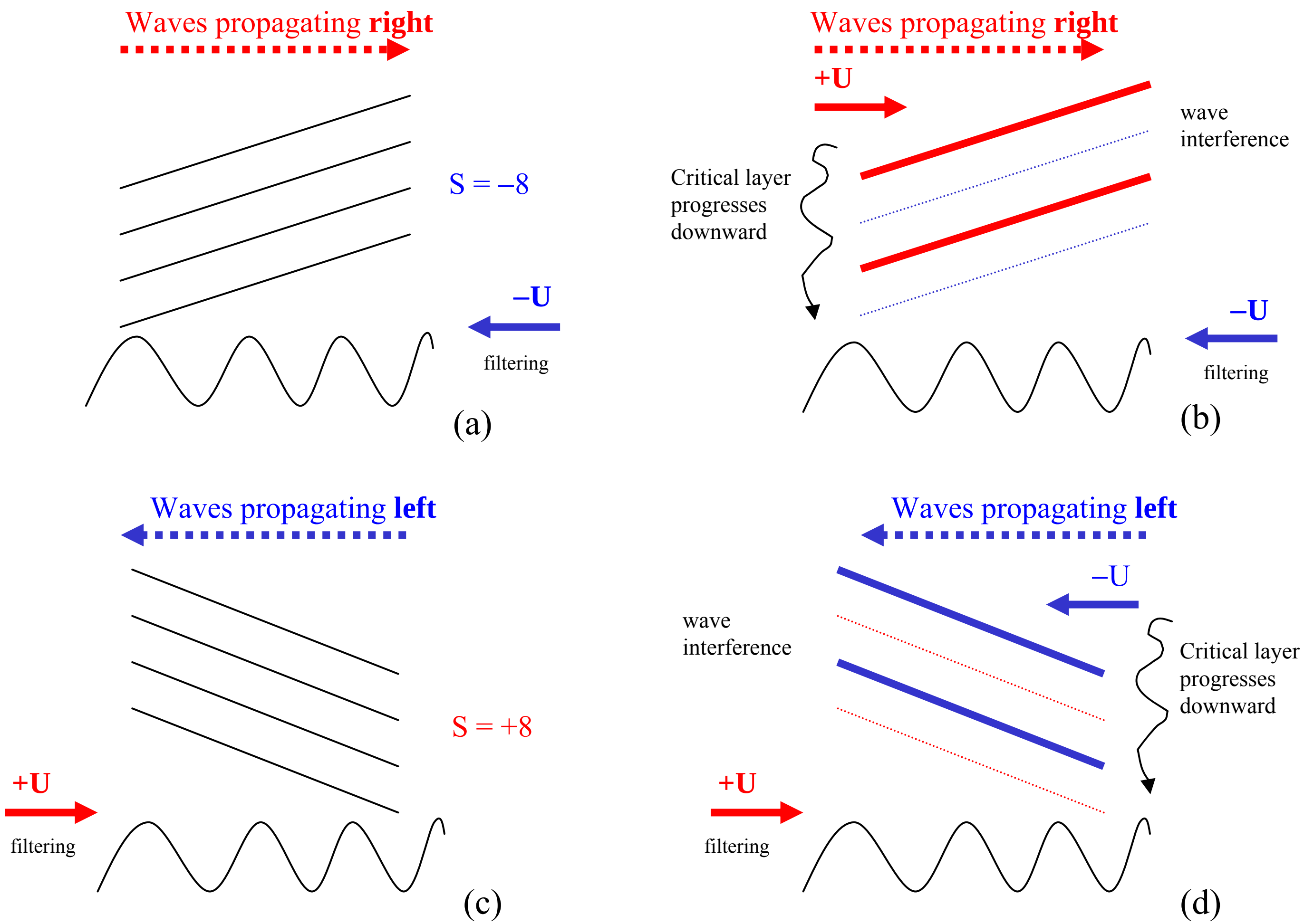

Generalized coordinate equations in density

$$\frac{\partial(\rho^* \overline{v^s}^k)}{\partial \overline{x}^k} = 0\ ,$$

$$\frac{dv^j}{d\overline{t}} = -\ \widetilde{G}_j^k \frac{\partial \pi'}{\partial \overline{x}^k} - g\frac{\rho'}{\rho_b}\delta_3{}^j + F^j + \mathcal{V}^j$$

$$\frac{d\rho'}{d\overline{t}} = -\overline{v^s}^k \frac{\partial \rho_e}{\partial \overline{x}^k} + \mathcal{H}\ .$$

```
Call dissip(. . .)
```

```
! Boussinesq in rho
! th means density perturbation
rhoinc=rh00
Gmod =-dth*g/rhoinc*astri
Gmodt=-dth*g/rhoinc*astrti
. . . Gmodt*th(i,j,k) . . .
```


ECMWF

Time-dependent coordinate transformation

$$\xi = \xi(x, y, z, t) := H_0 \frac{z - z_s(x, y, t)}{H(x, y, t) - z_s(x, y, t)}$$

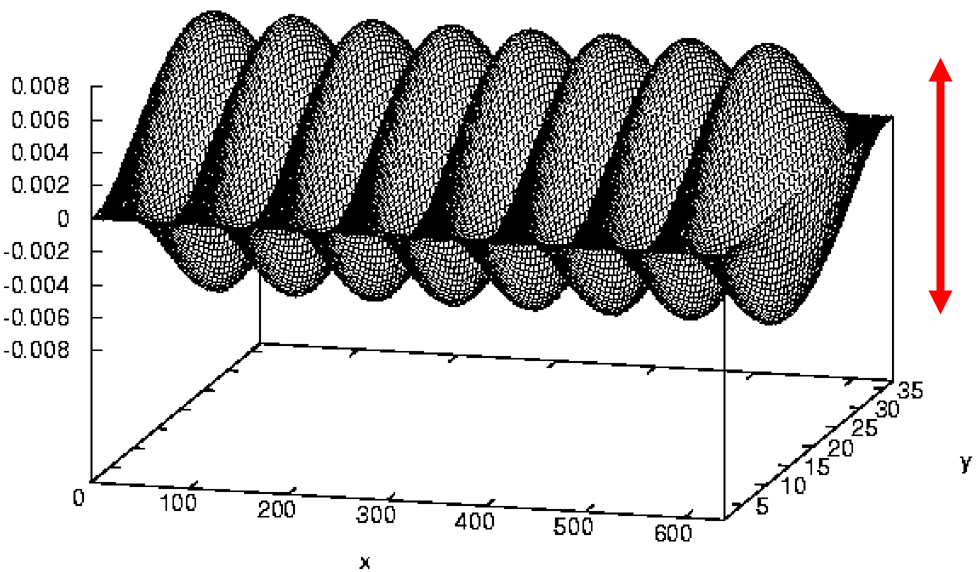

Time dependent boundaries

Wedi and Smolarkiewicz,
J. Comput. Phys 193(1) (2004) 1-20

$$z_s(x, y, t) = \epsilon \sin(\frac{\pi}{L_y} y) \sin(\frac{2\pi s}{L_x} x) \sin(\omega_0 t)$$

ECMWF

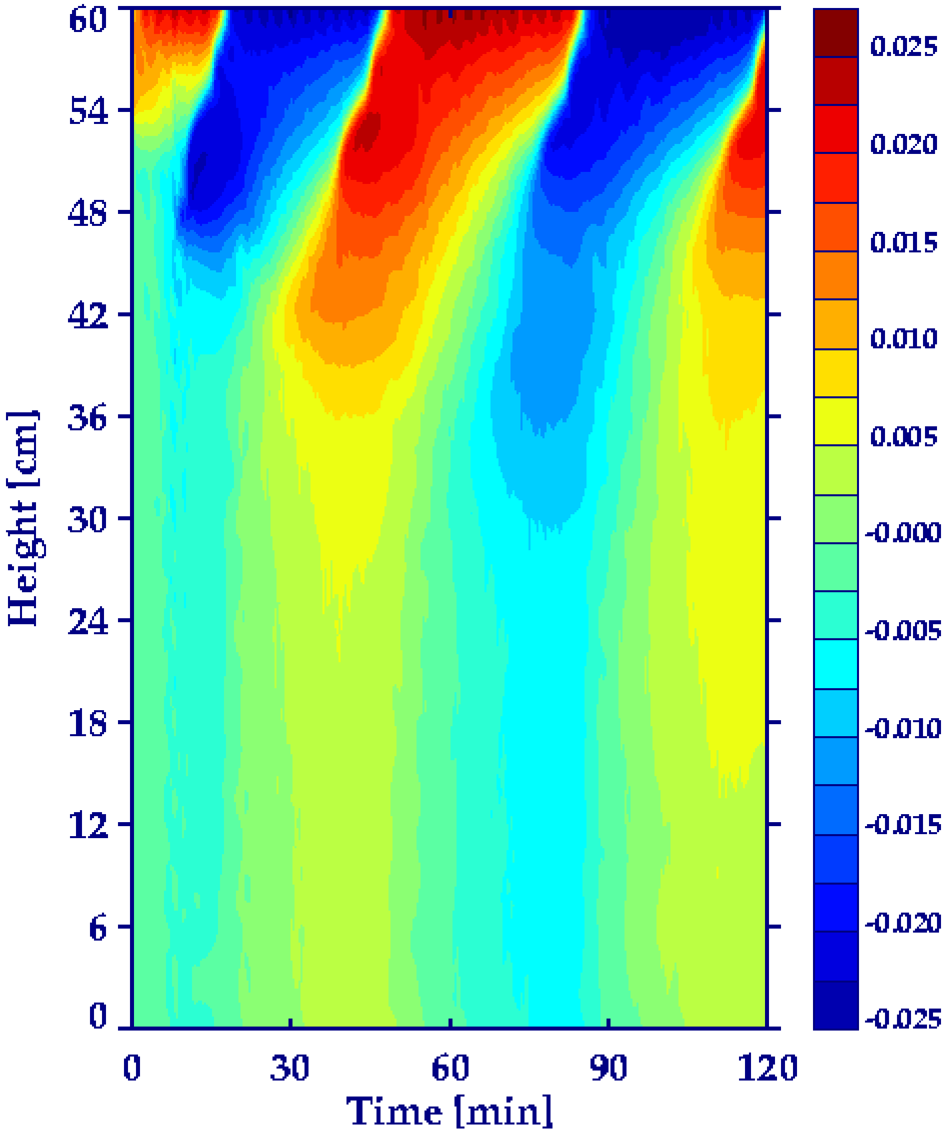

Time – height cross section of the mean flow U in a 3D simulation

Animation

ECMWF

Cylindrical coordinates

$$\hat{x} = R - a$$

$$\hat{y} = R\alpha$$

$$\hat{z} = z$$

$$\Gamma = 1 + \frac{\hat{x}}{a}$$

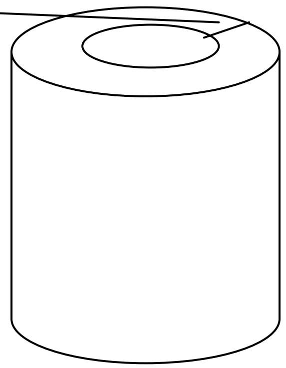

```
gmm(i,j,k)=rdsi*(x(ia)+rds)
```

```
      dya=(360./180.)*pi/float(m-1)
      dy=rds*dya
c ----  specify computational grid
      do 1 i=1,n
       . . .
       else if (icylind.eq.1) then
        x(i)=(i-1)*dx        ! cylindrical (m)
       . . .
1 continue
      do 2 j=1,m
       . . .
       else if (icylind.eq.1) then
        y(j)=(j-1)*dya       ! cylindrical (radians)
       end if
    2 continue
      do 3 k=1,l
        z(k)=(k-1)*dz
    3 continue
      zb=z(l)
      zb=dz*(l-1)
```

Energy budget

call energy(...)

(Wedi, Int. J. Numer. Fluids, 2006)

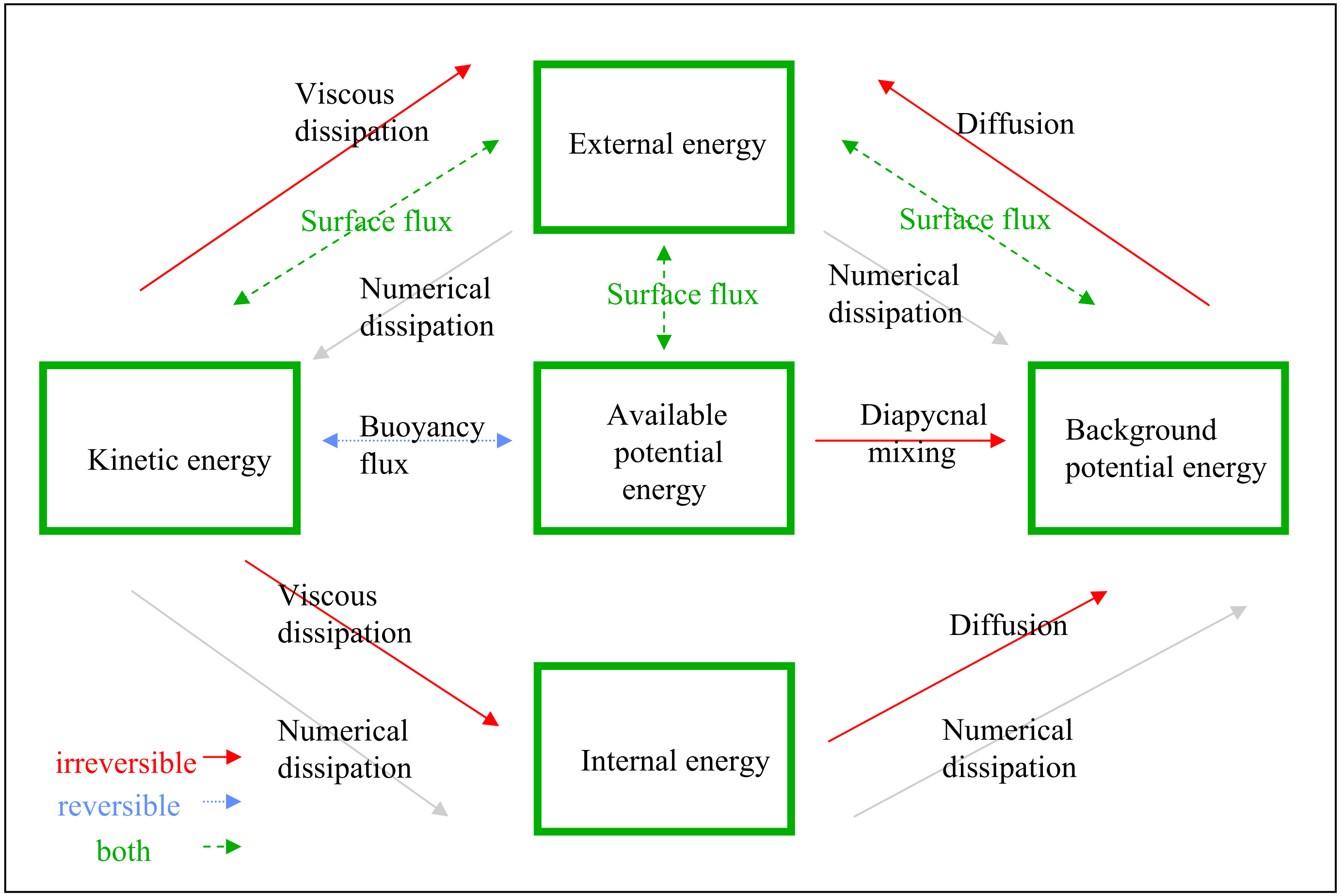

adapted from Winters et. al. JFM 289 115-128 (1995)

ECMWF

Energy

kinetic

$$E_k = \frac{\rho_0}{2} \int_V (u^2 + v^2 + w^2) dV.$$

potential

$$E_p = g \int_V \rho' z dV.$$

available potential

$$E_p = E_b + E_a.$$

background potential

$$E_b = \int_V gz(\rho_* - \rho_e) dV$$

Energy rates

irreversible

reversible

viscous dissipation

$$\frac{d}{dt}E_k = -\oint_S \left[p'\mathbf{v} + \frac{\rho_0}{2}\mathbf{v}(u^2+v^2+w^2) - \mathbf{v}\cdot\boldsymbol{\tau}\right]\cdot\hat{\mathbf{n}}dS - \int_V g\rho' w dV - \mathcal{D}.$$

surface fluxes

buoyancy

$$\frac{d}{dt}E_p = -\oint_S gz\rho\mathbf{v}\cdot\hat{\mathbf{n}}dS + \int_V g\rho' w dV + \kappa g\oint_S z\nabla\rho\cdot\hat{\mathbf{n}}dS - \kappa g A_{xy}(<\rho_{top}>_{xy} - <\rho_{bottom}>_{xy}).$$

diffusion

$$\frac{d}{dt}E_b = S_{adv} + S_{diff} - \kappa g\int_V \left(\frac{d\rho_*}{dz}\right)^{-1}|\nabla\rho|^2 dV$$

diapycnal mixing

Reversible rates (Eulerian)

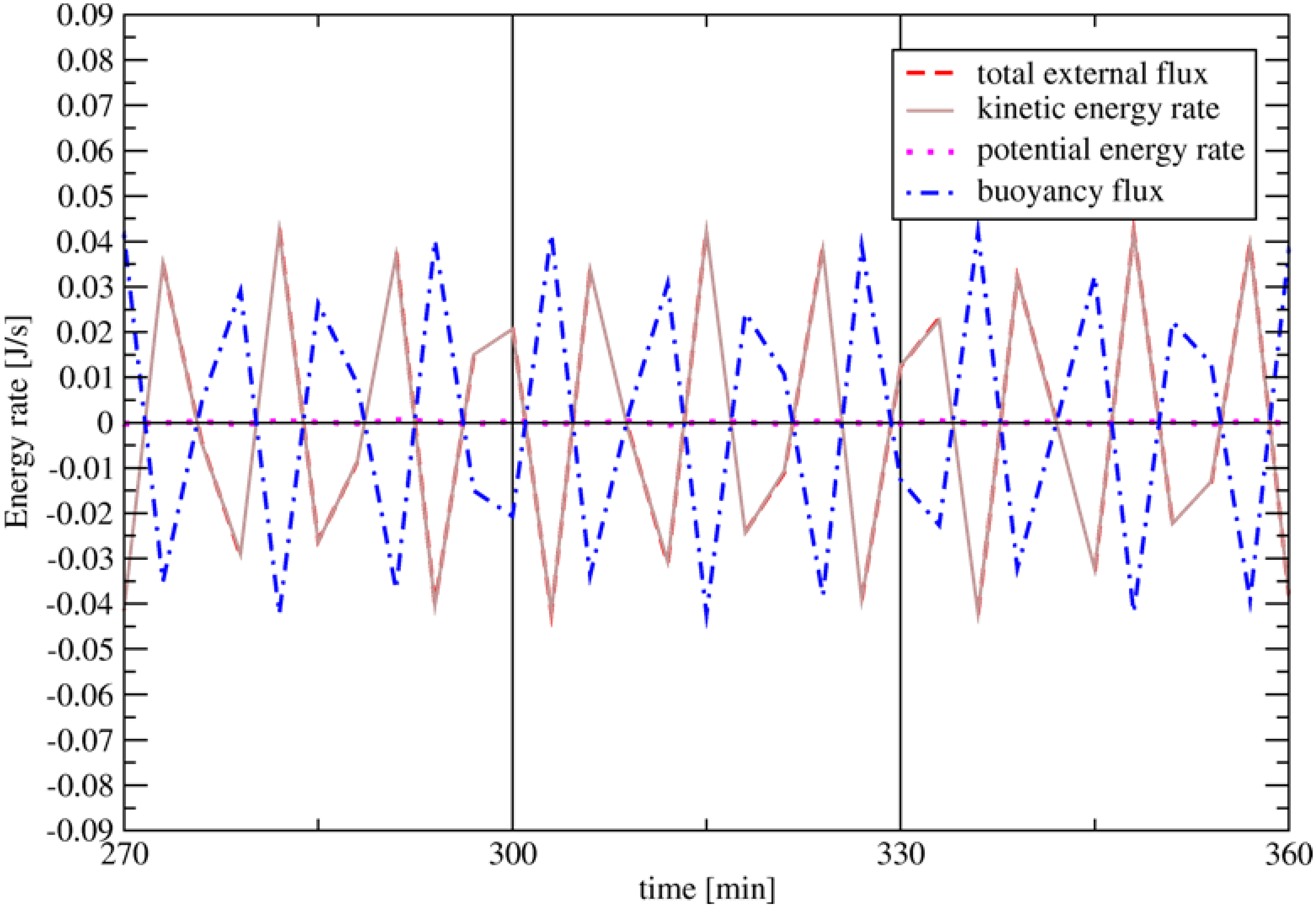

Kinetic energy (Eulerian)

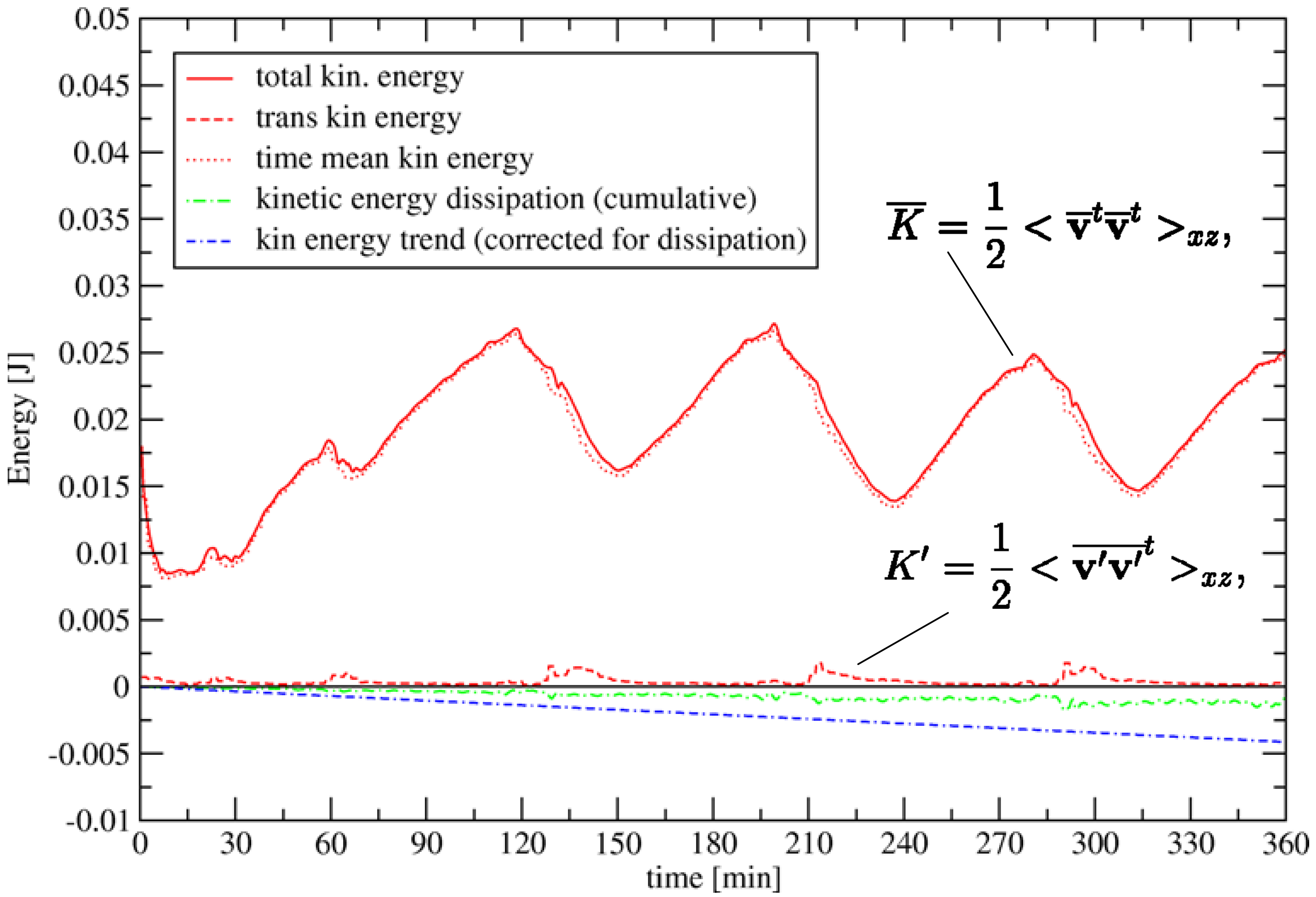

Pot. energy (Eulerian)

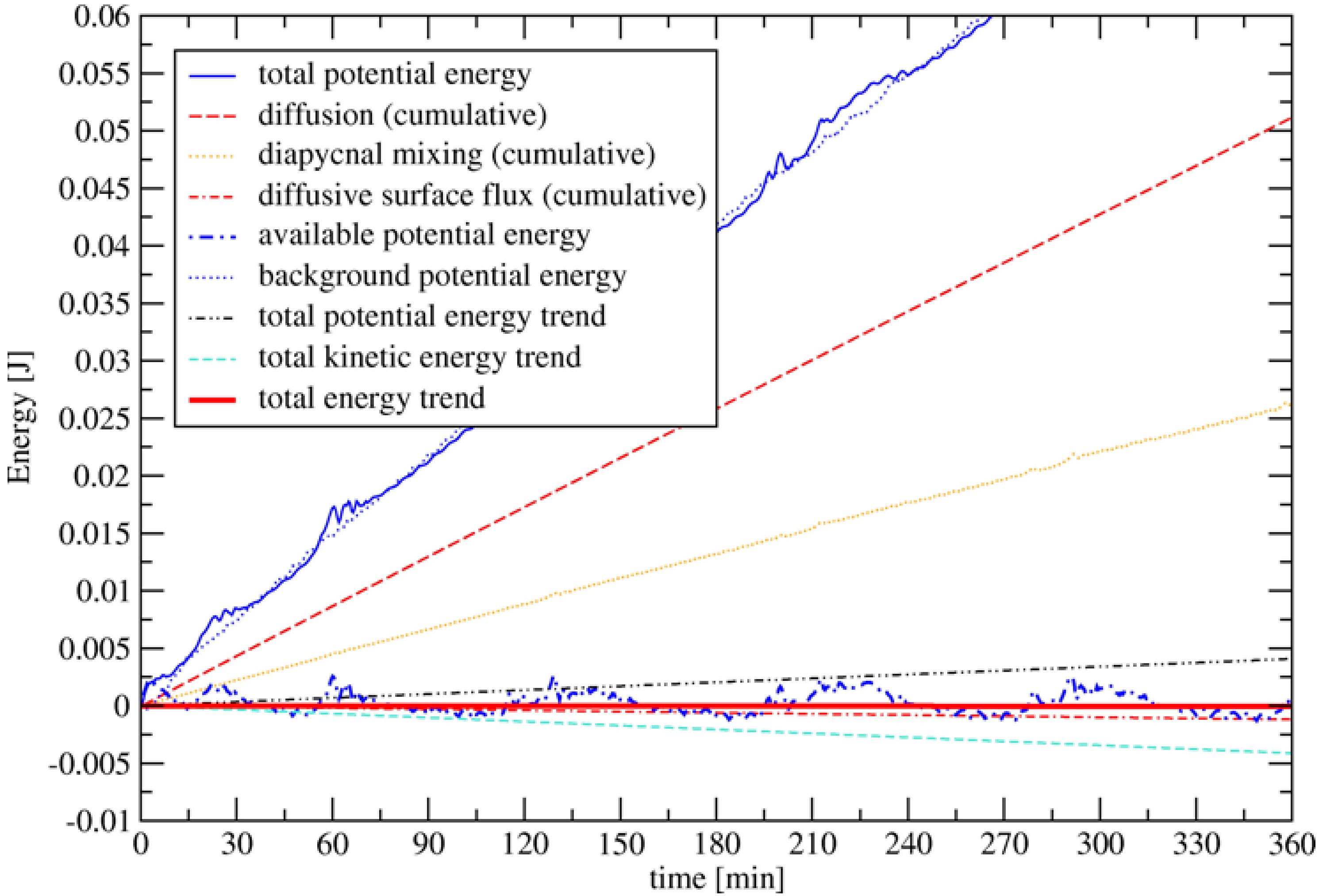

ECMWF

Pot. energy (semi-Lagrangian)

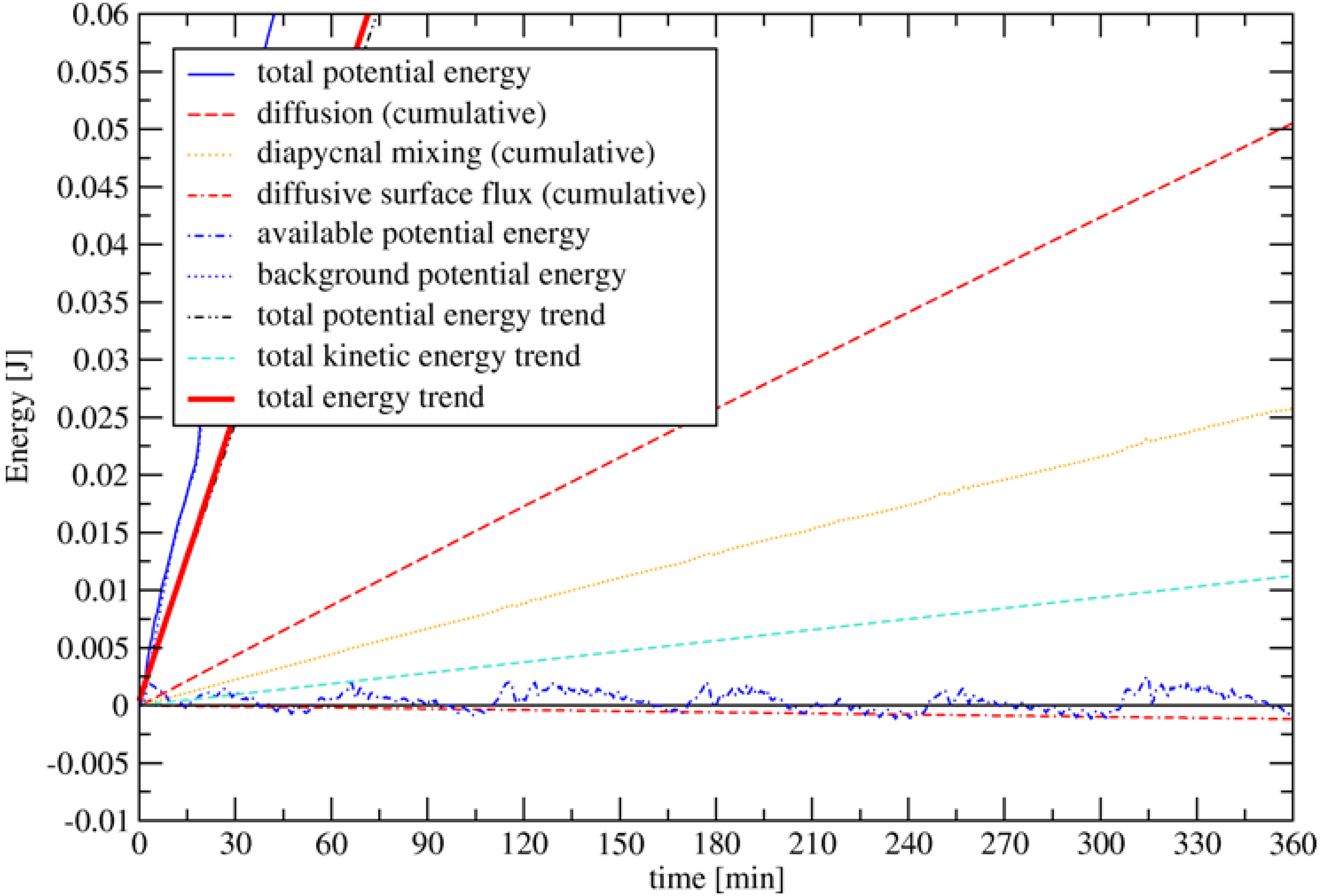

ECMWF

Flow evolution

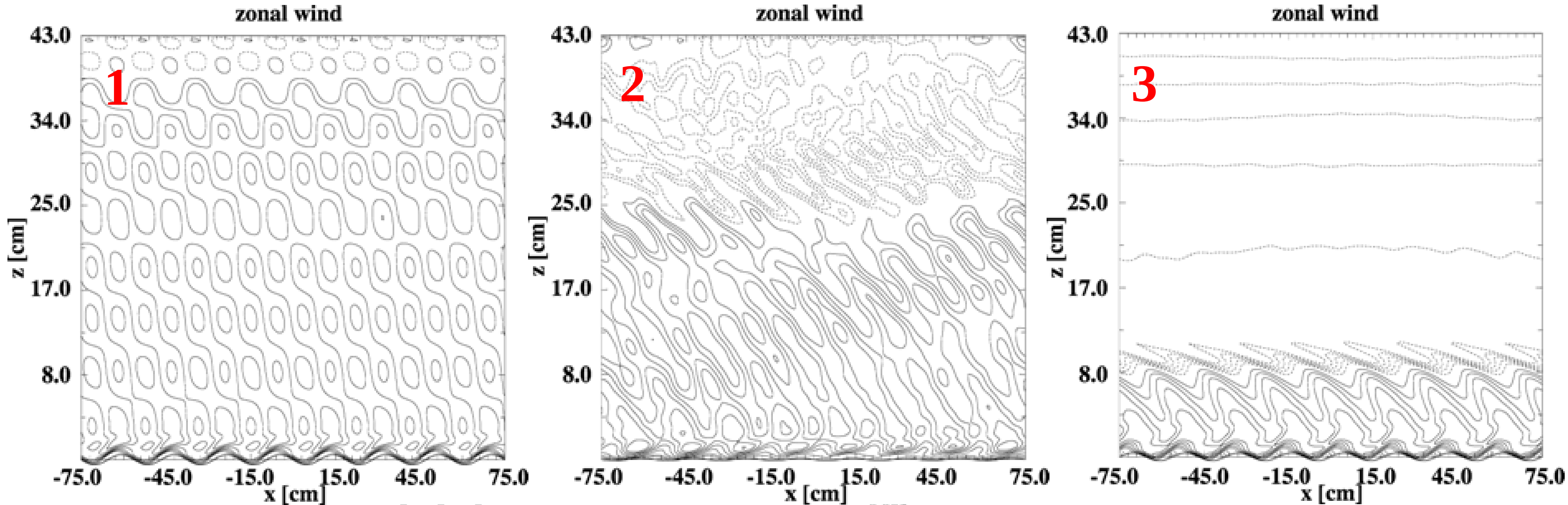

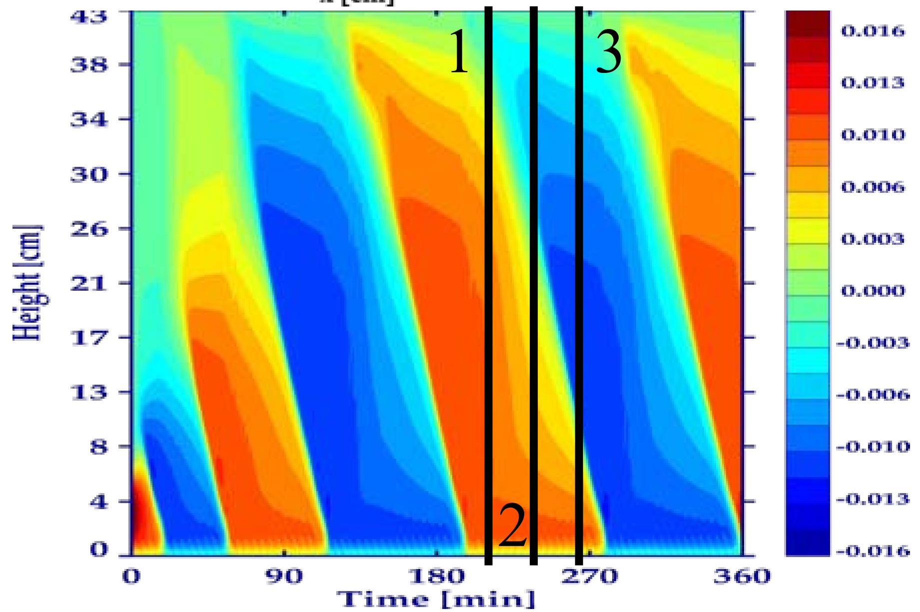

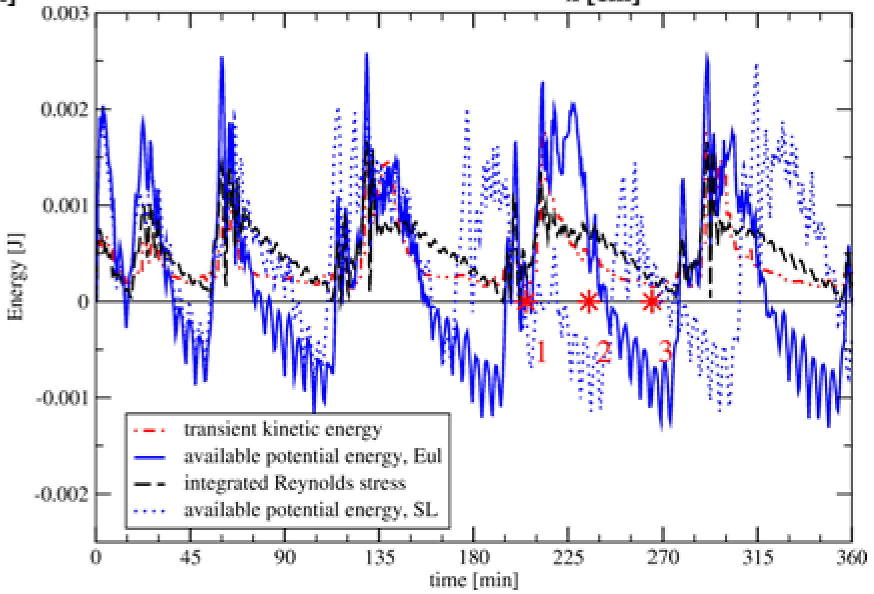

“Transient” energies

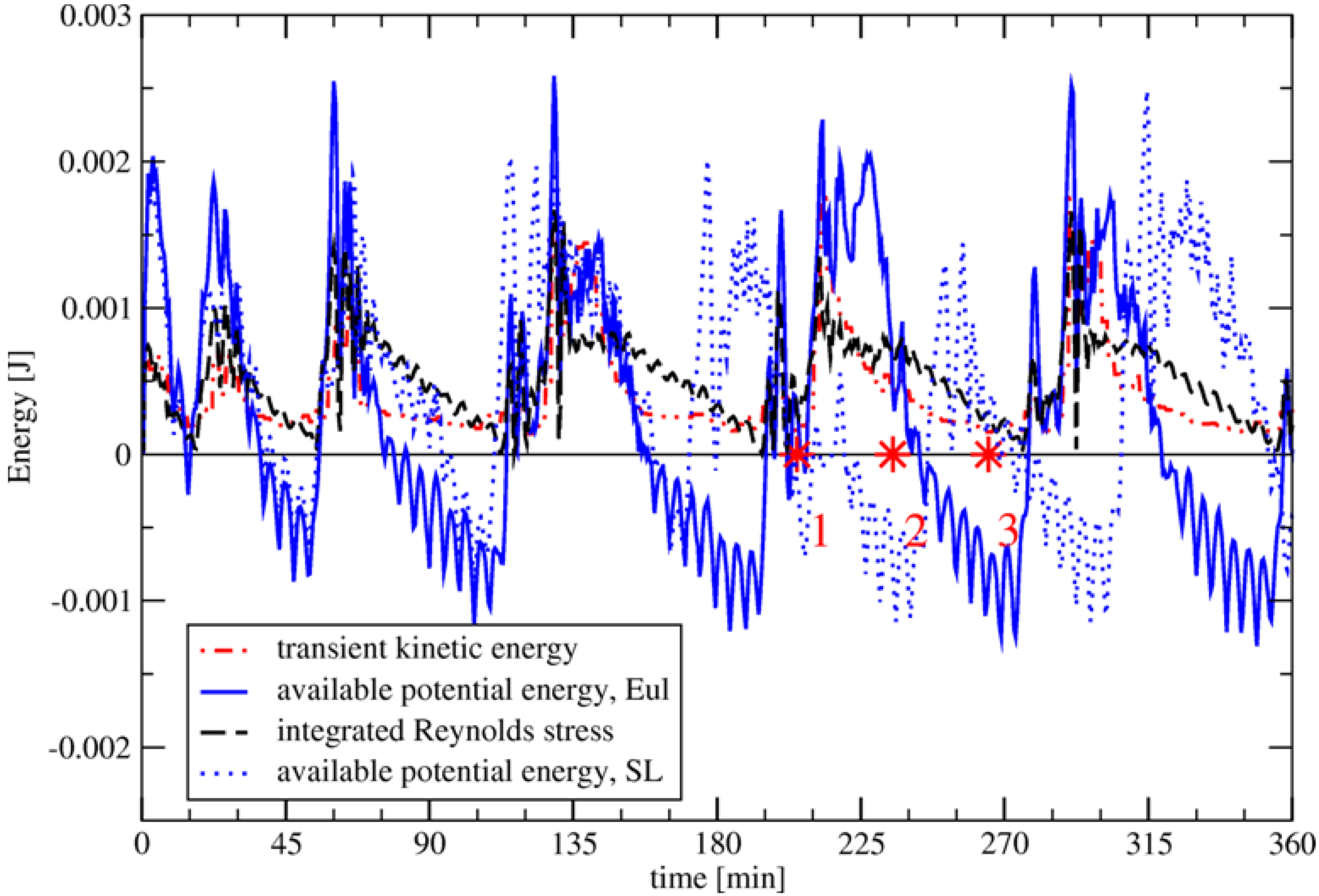

Viscous simulation

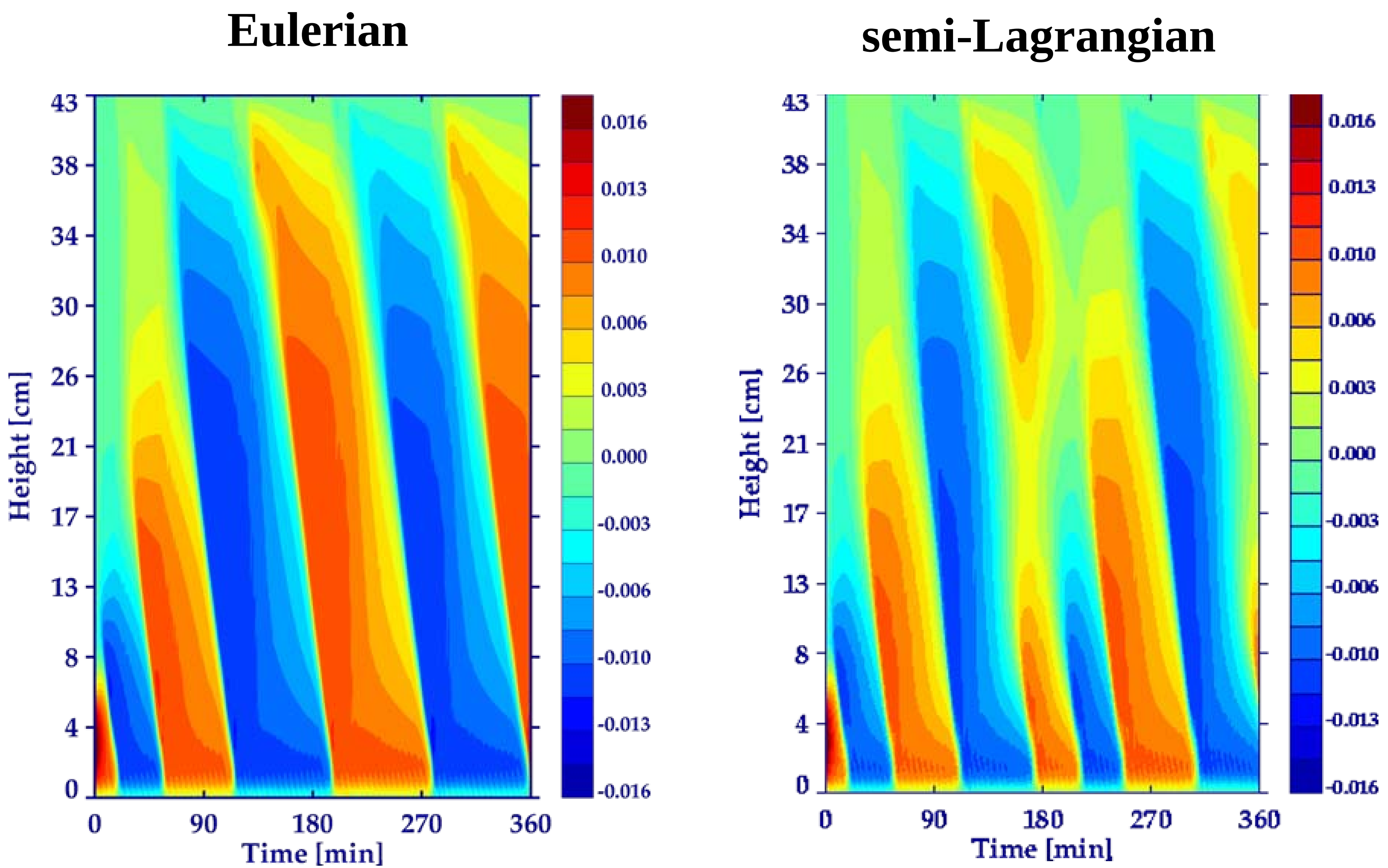

ECMWF

Inviscid simulation

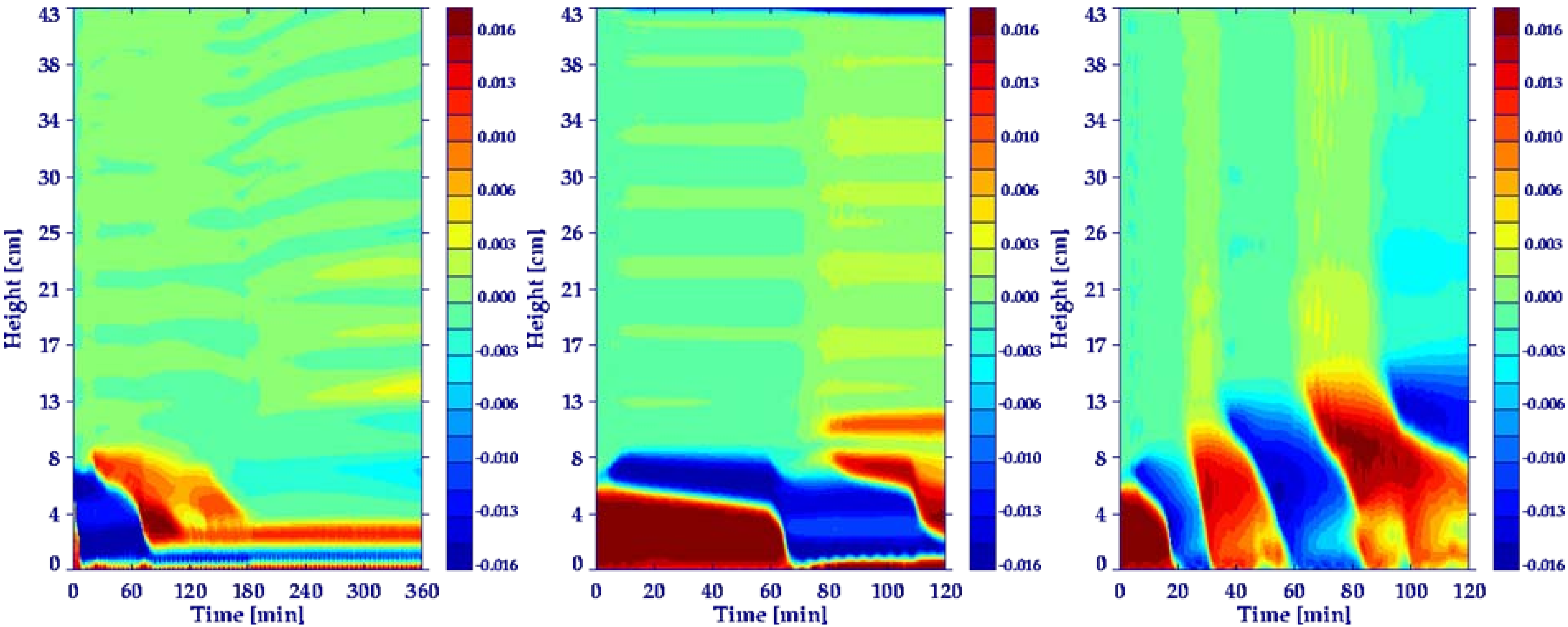

Eulerian
St=0.36, n=640
top absorber

Eulerian
St=0.25, n=384
top rigid, freeslip

semi-Lagrangian
St=0.25, n=384
top rigid, freeslip

Numerical realisability

Influence on the period and the vertical extent of the resulting zonal mean zonal flow changes

- **Lower horizontal resolution results in increasing period (~16 points per horizontal wavelength still overestimates the period by 20-30%)**
- **Lower vertical resolution results in decreasing period and earlier onset of flow reversal as dynamic or convective instabilities develop instantly rather than previously described wave-wave mean flow interaction *(need ~10-15 points per vertical wavelength, <5 no oscillation observed)***
- **First or second order accurate *(e.g. rapid mean flow reversals with 1st order upwind scheme)***
- **A low accuracy of pressure solver may result in spurious tendencies with a magnitude similar to physical buoyancy perturbations and are due to the truncation error of the Eulerian scheme; equally explicit vs. implicit formulation of the thermodynamic equation results in distorted longer mean flow oscillation *(explicit may be improved by increasing the vertical resolution)***
- **Choice of advection scheme *(flux-form Eulerian more accurate)***
- **Upper boundaries and stratification changes *(may catalyze the onset of flow reversal; also in 2D Boussinesq experiments due to wave reflection, in atmospheric conditions also changing wave momentum flux with non-Boussinesq amplification of gravity waves)***

Time dependent lateral meridional boundaries

- **Beta-plane virtual laboratory**
- **Zonally-periodic equatorial β-plane channel**
- **Constant ambient flow U=0.05m/s**
- **Time-dependent lateral (y-)boundaries, using the continuous coordinate transformation (k_x = 6 or 12, $\omega_1=2\pi/100s$, $\omega_2=2\pi/120s$)**

$$\bar{x} = E(x,y,t) = x$$

$$\bar{y} = D(x,y,t) = y_0 \left(\frac{y - y_s(x,y,t)}{y_t(x,y,t) - y_s(x,y,t)} \right)$$

$$y_s(x,t) = 0.5 y_{s0}(sin(k_x x - \omega_1 t) + sin(k_x x - \omega_2 t))$$

Time dependent lateral meridional boundaries

Sizes and setup inspired by "Laboratory modeling of topographic Rossby normal modes" (Pierini et al., Dyn. Atmos. Ocean 35, 2002)

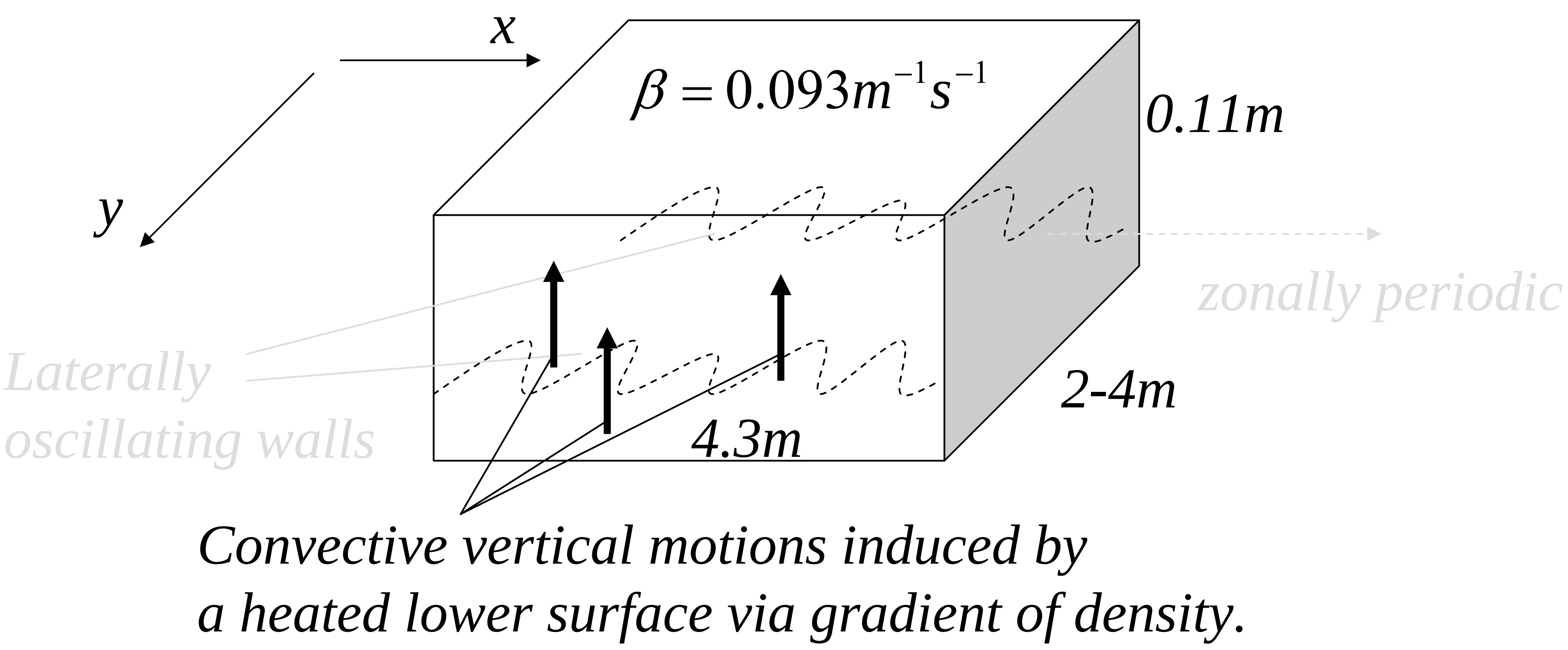

MJO-like eastward propagating anomalies

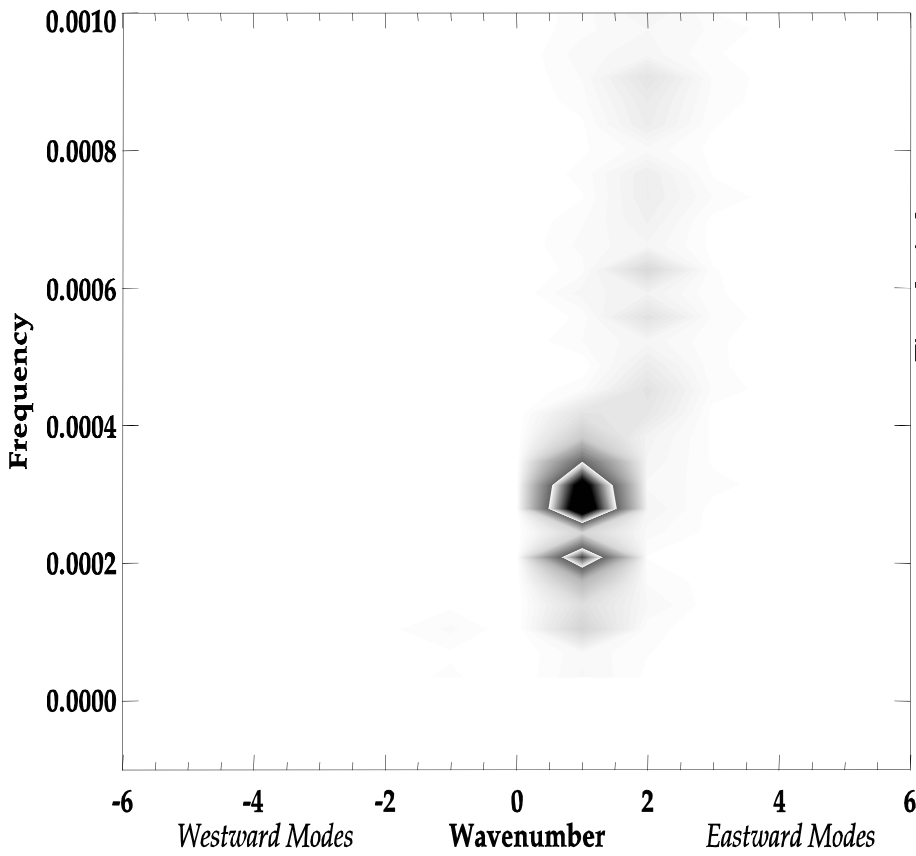

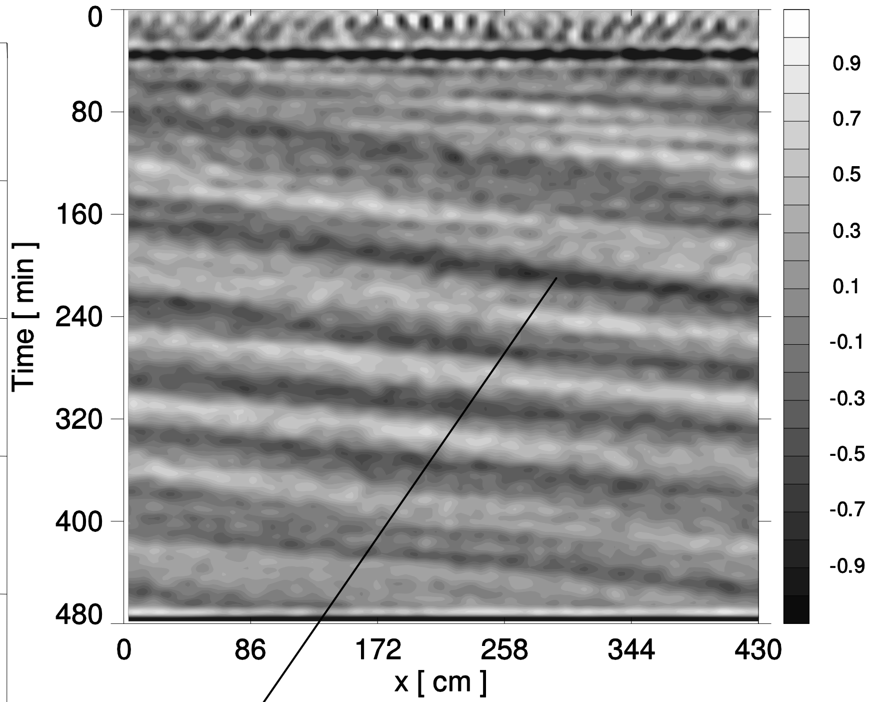

Velocity potential anomalies propagate eastward as a result of the lateral meridional boundary forcing.

MJO-like eastward propagating anomalies

horizontal structure

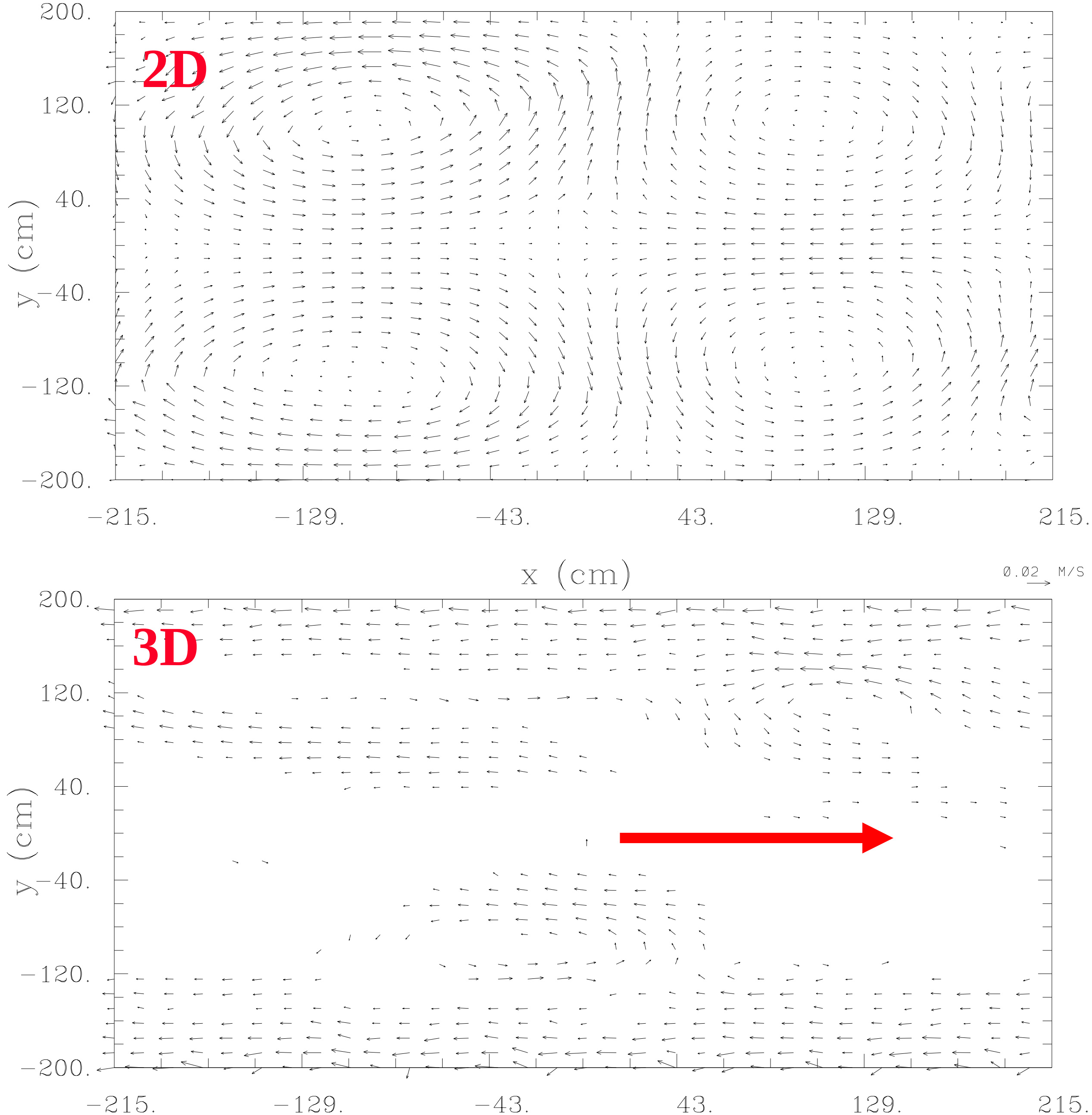

ECMWF

Local- and synoptic-scale simulations on the sphere ...

The size of the computational domain is reduced without changing the depth or the vertical structure of the atmosphere by changing the radius ($a < a_{Earth}$)

(Smolarkiewicz et al, 1998; Wedi and Smolarkiewicz, 2008)

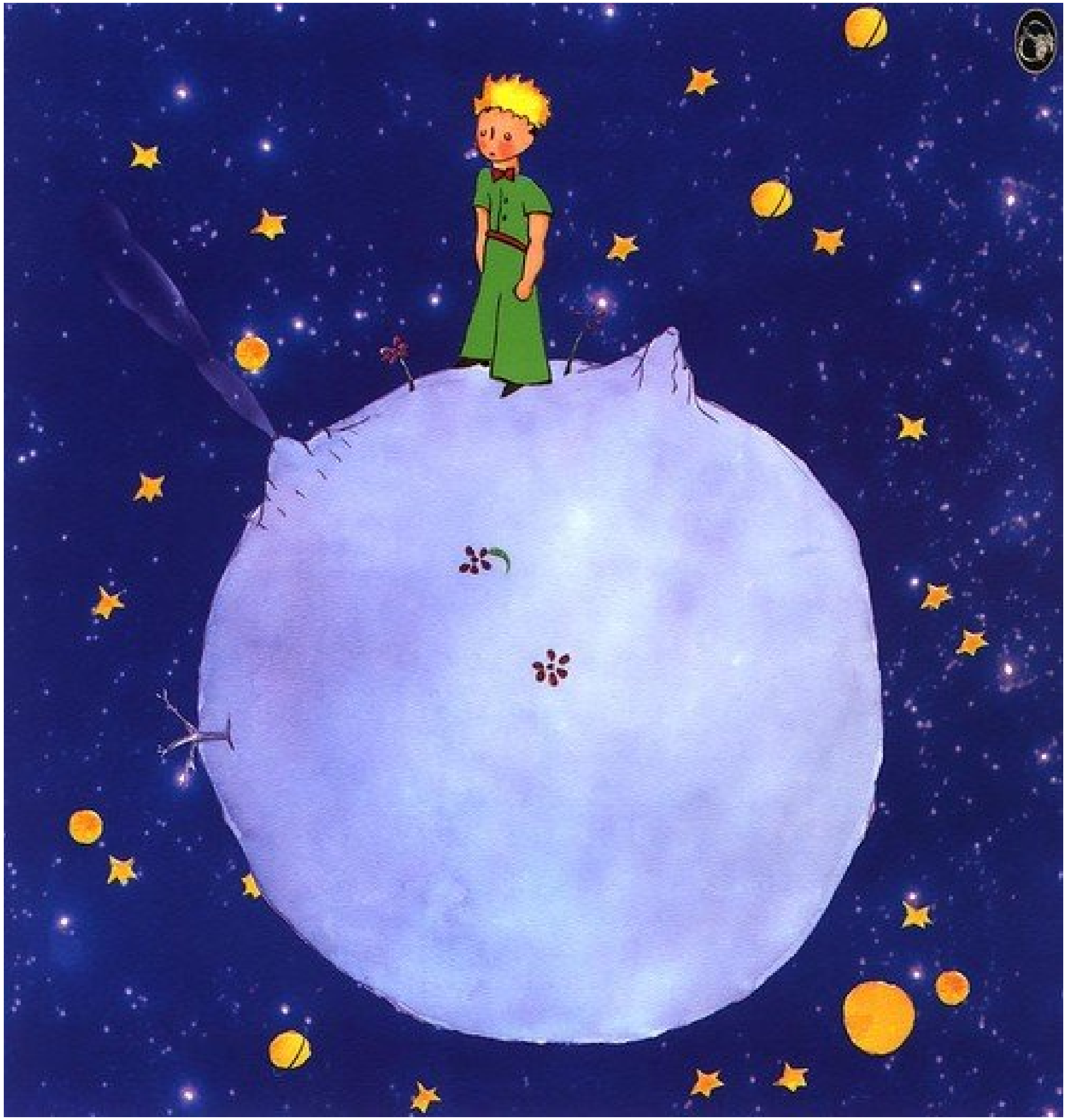

Spherical coordinates

$$\hat{x} = a\lambda$$

$$\hat{y} = a\phi$$

$$\hat{z} = r - a$$

$$\Gamma = 1 + \frac{\hat{z}}{a}$$

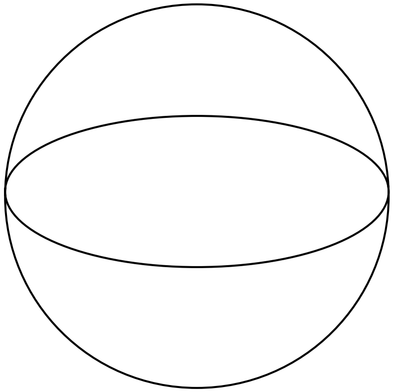

```
         gmm(i,j,k)=1+isphere*zcrl/rds


        if(isphere.eq.1) then                    ! Specify ONLY dz in blanelas
         dxa=(360./180.)*pi/float(n-1)            ! full zonal extent :radians
         dya=(160./180.)*pi/float(m)              ! full meridional extent
         dx=rds*dxa                               ! meters
         dy=rds*dya
         endif . . .
        do 1 i=1,n
         if(isphere.eq.1) then
          x(i)=(i-1)*dxa                          ! sphere (radians)
         end if
      1 continue
        do 2 j=1,m
          if(isphere.eq.1) then
c          y(j)=-pih+(j-0.5)*dya                  ! sphere (radians)
           y(j)=-(160.0/180.0)*pi+(j-0.5)*dya
          end if
      2 continue
```

Comparison to nonhydrostatic IFS

- **Based on the limited-area model ALADIN-NH *(Bubnova et al 1995, Benard et al 2004a,b, Benard et al 2005)* and coded into the IFS by Météo-France and its ALADIN partners.**
- **The hydrostatic shallow atmosphere framework at ECMWF has been gradually extended to the deep-atmosphere fully compressible equations within the existing spectral two-time-level semi-implicit semi-Lagrangian code framework.**
- **Mass-based vertical coordinate *(Laprise, 1992),* equivalent to hydrostatic pressure in a shallow, vertically unbounded planetary atmosphere.**

Quasi two-dimensional orographic flow with linear vertical shear

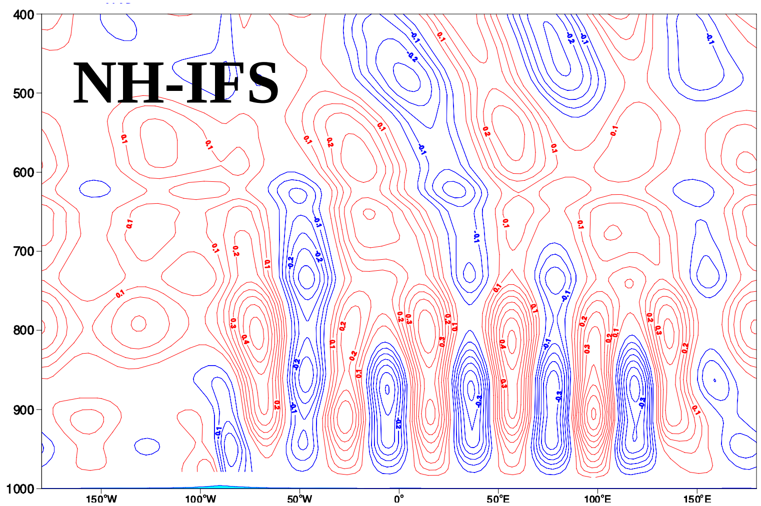

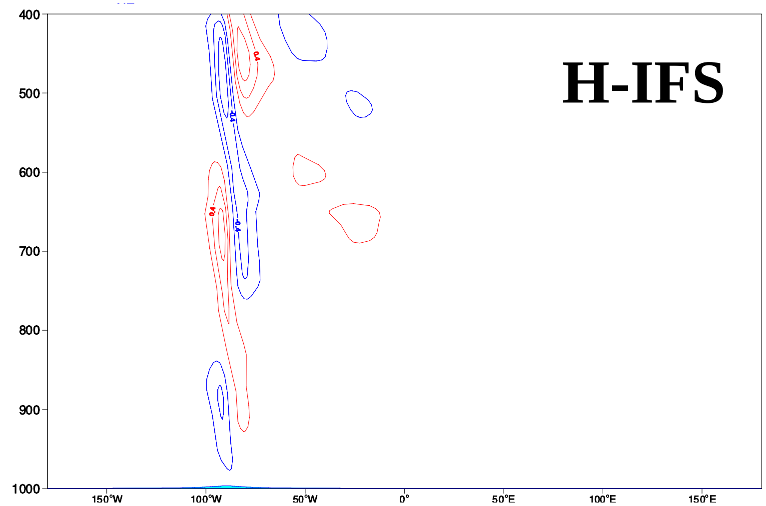

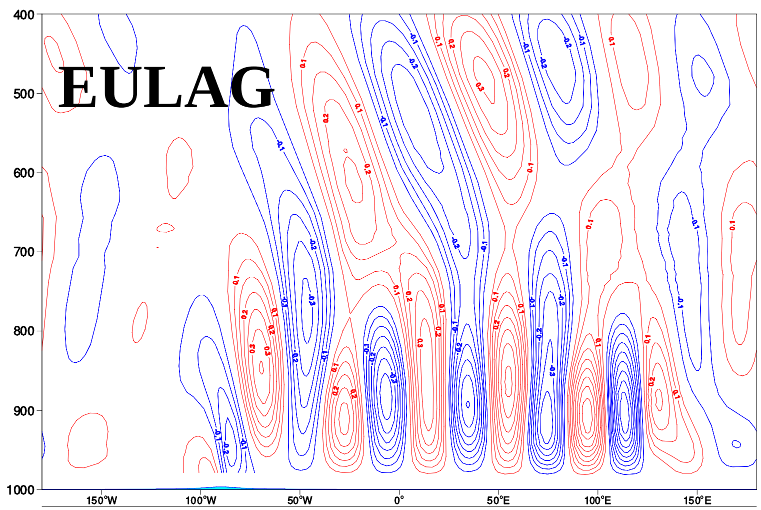

The figures illustrate the correct horizontal (NH) and the (incorrect) vertical (H) propagation of gravity waves in this case (Keller, 1994). Shown is vertical velocity.

Non-linear critical flow past a three-dimensional hill *(Grubisic and Smolarkiewicz, 1997)*

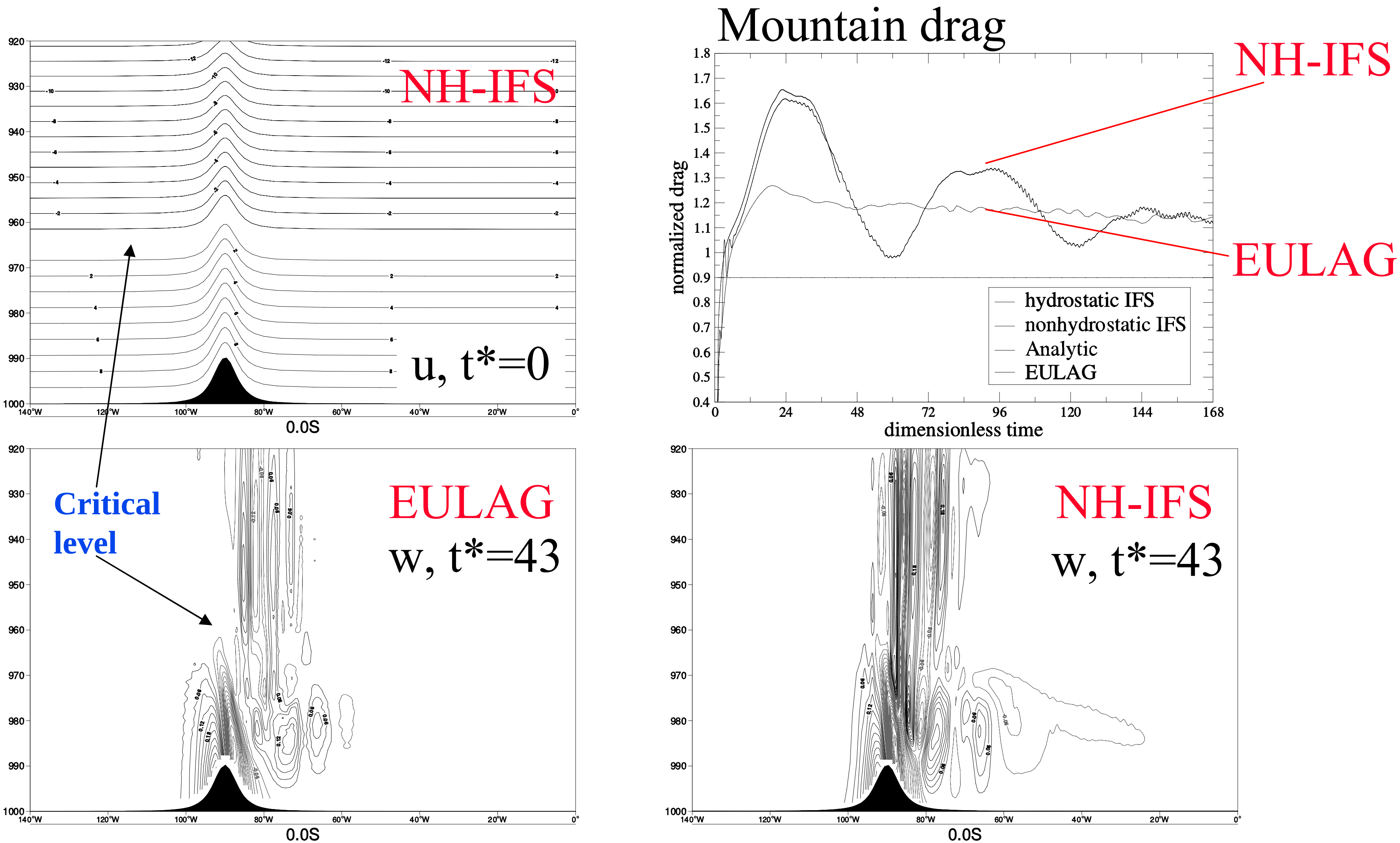

Convective motion (3D bubble test)

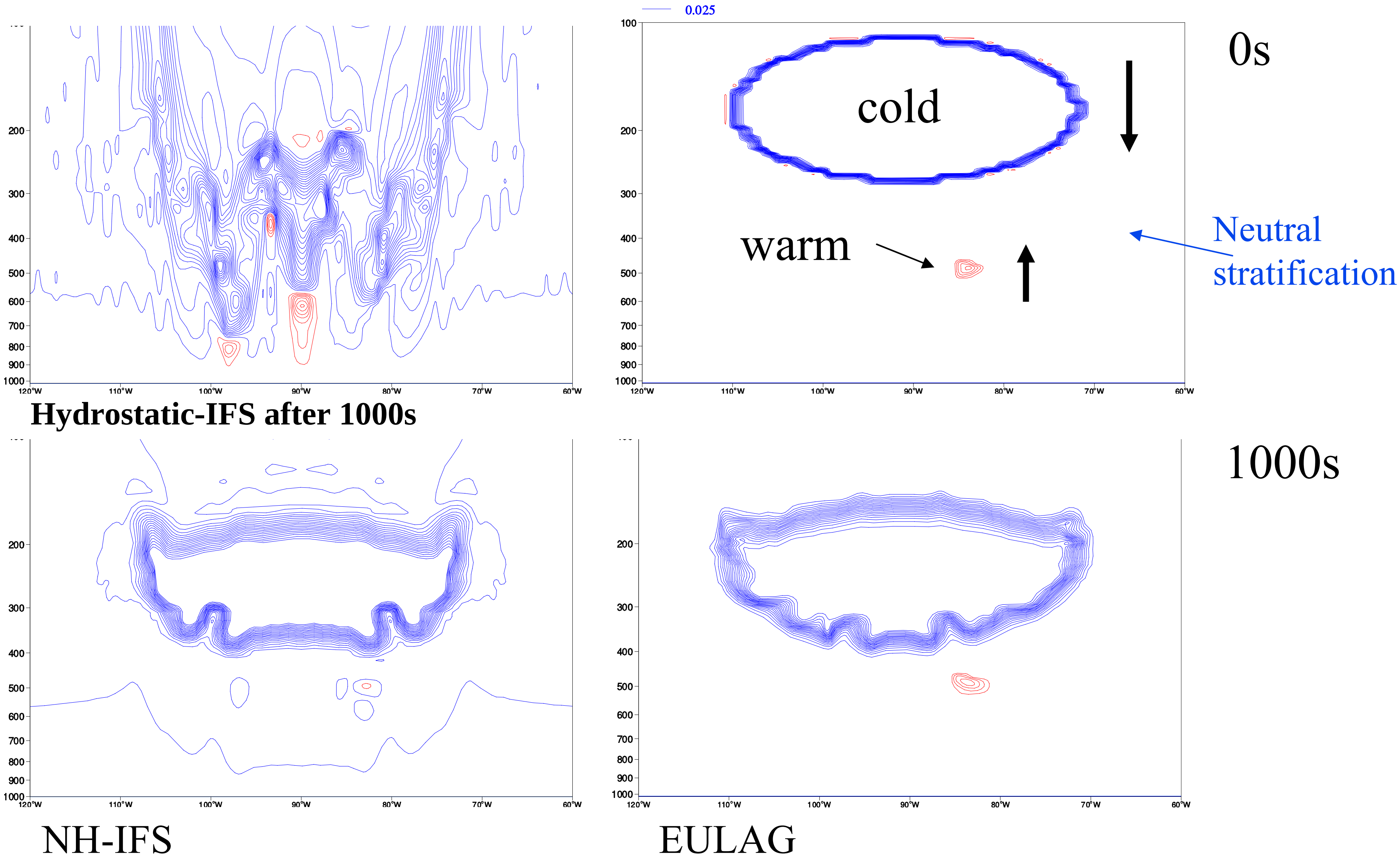

Convective motion (3D bubble test)

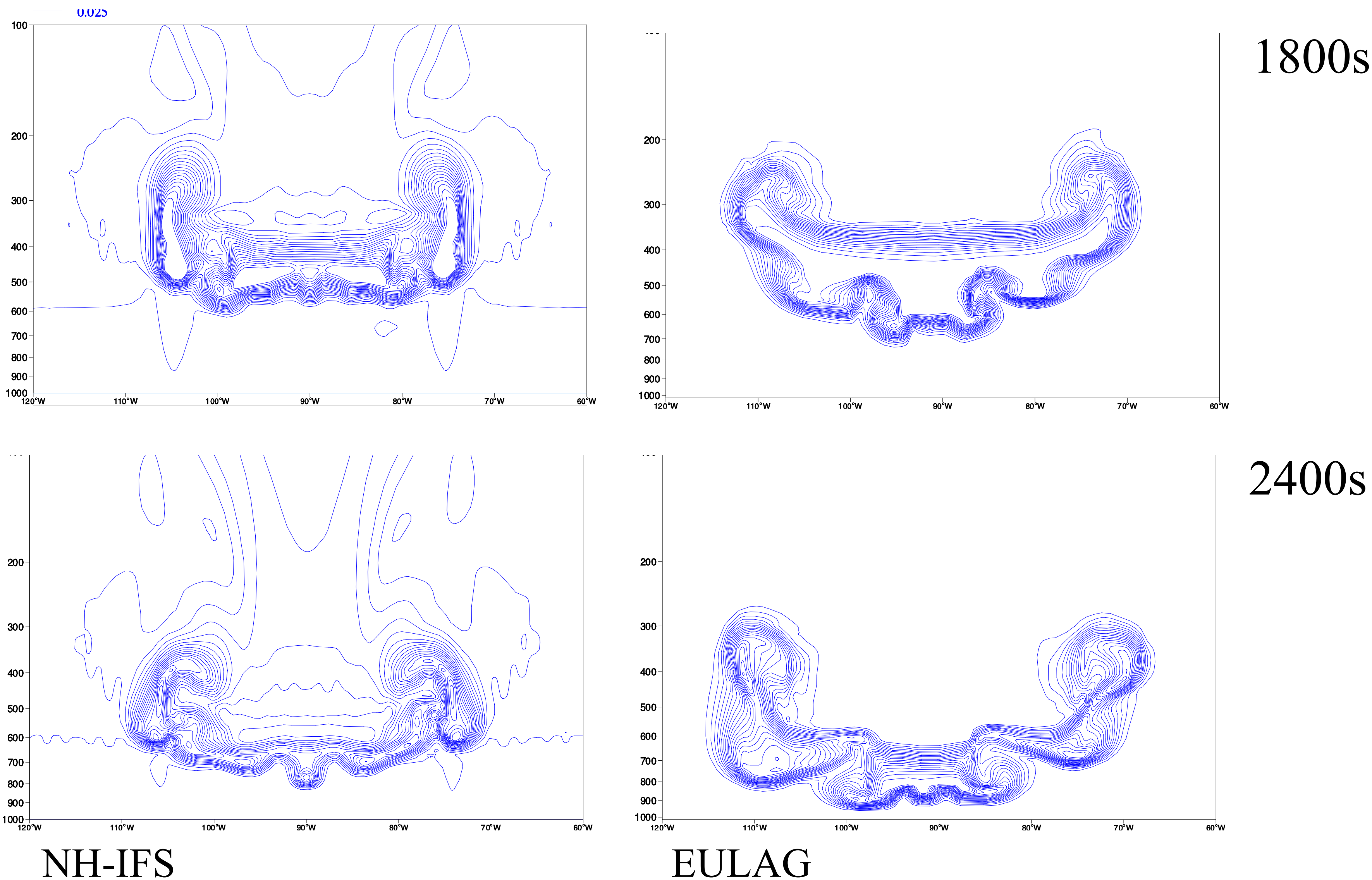

ECMWF

Held-Suarez ‘climate’ on reduced-size planet

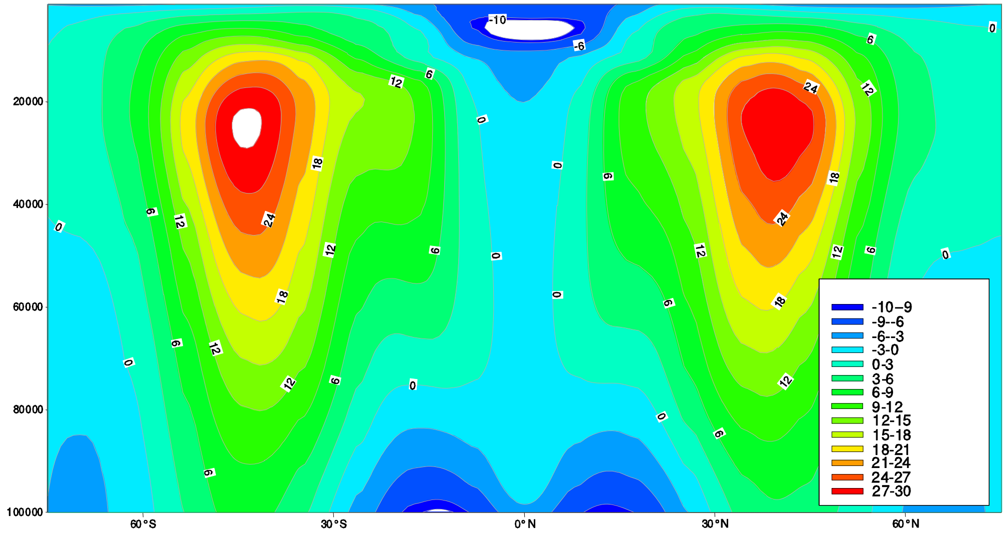

NH-IFS

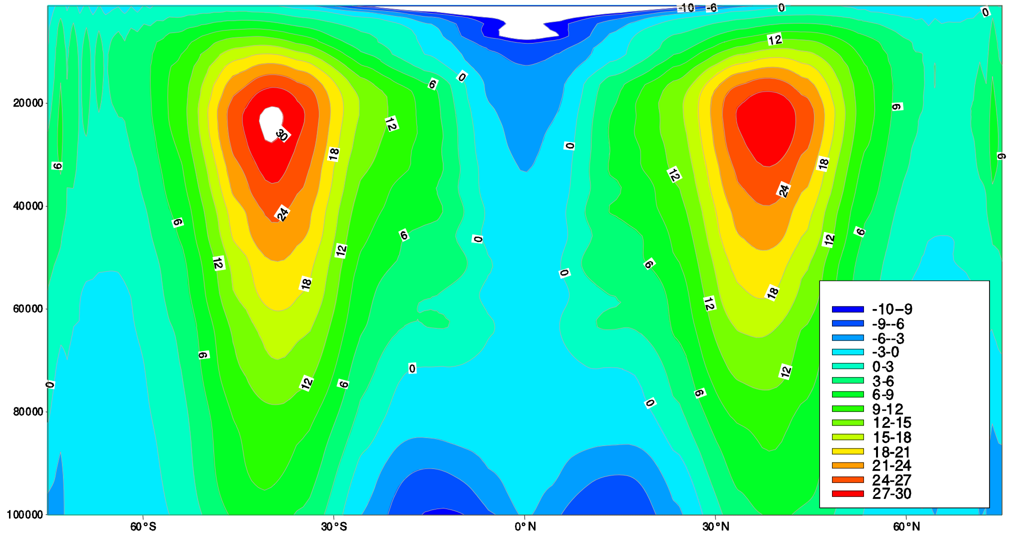

EULAG

$R=0.1R_{Earth}$, $T_L159L91$

Equivalent to

$\Delta x = 12.5$ km

ECMWF

Spectra of horizontal kinetic energy from the HS benchmark

$a=a_E$; $a=a_E/10$

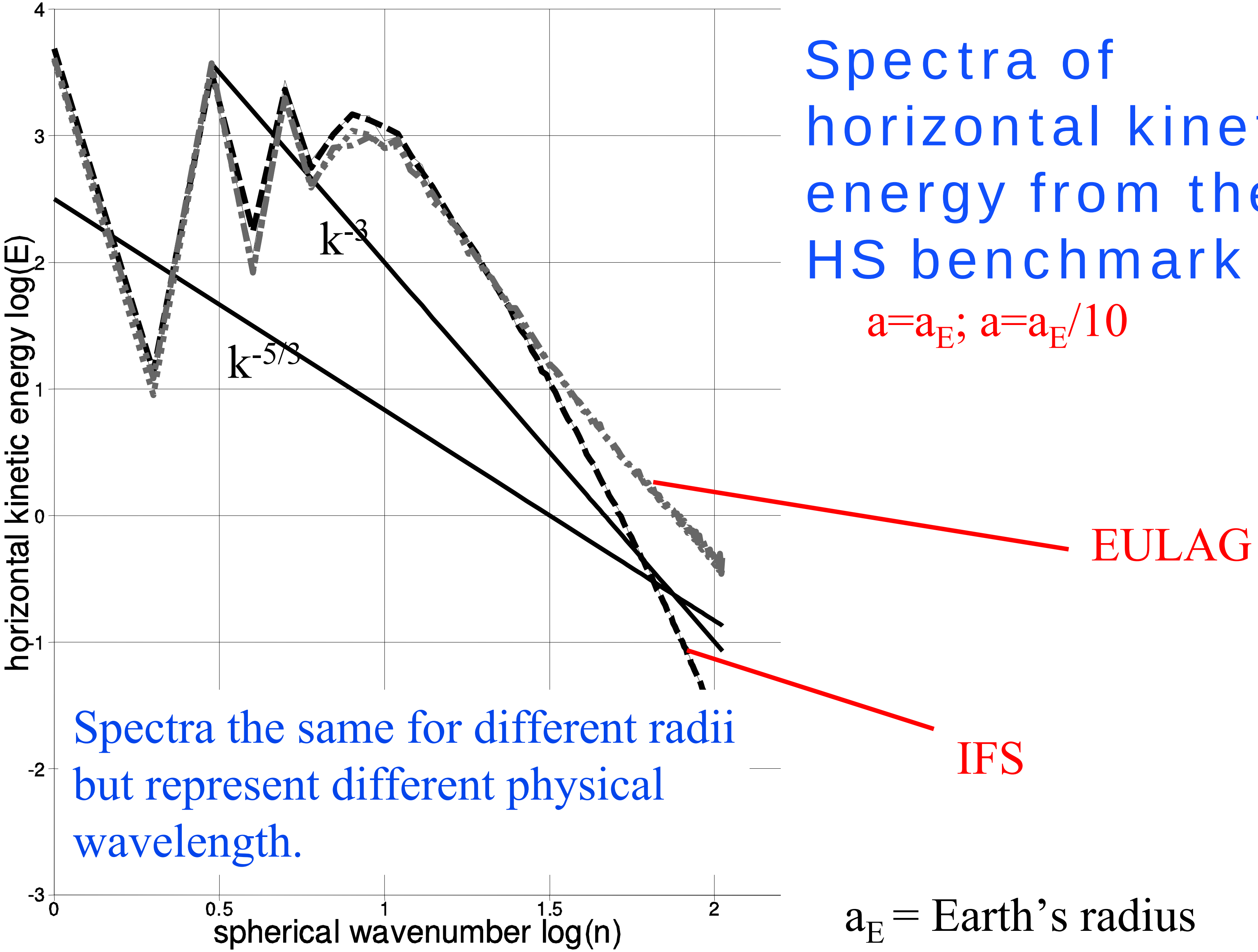

Spectra the same for different radii but represent different physical wavelength.

a_E = Earth's radius

ECMWF

Spectra for different EULAG options

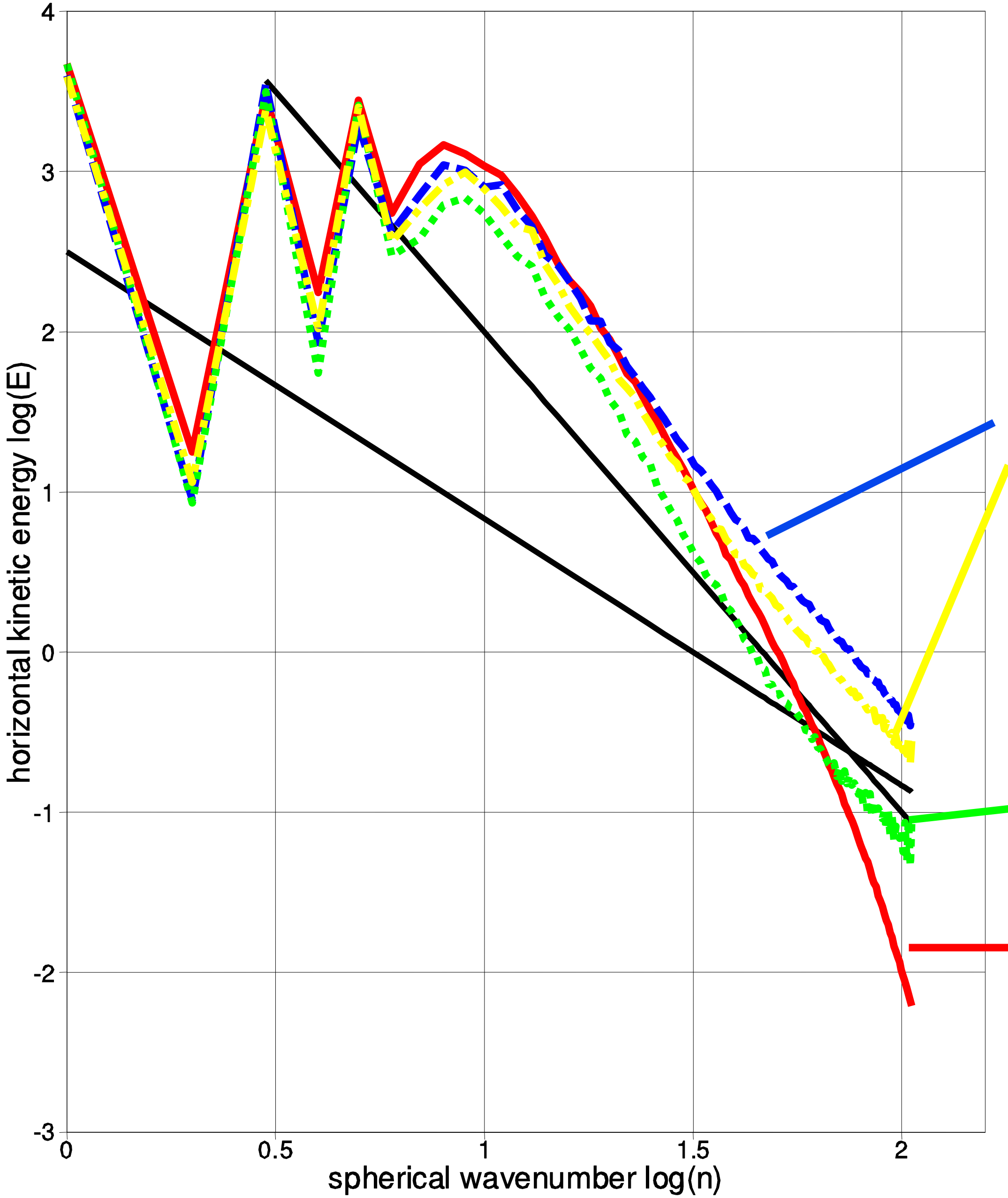


```
#if (J3DIM == 1)
if(iflg.ge.2.and.iflg.le.5) then
call mpdatm3(xd1,xd2,xd3,xf,d,iflg)
else
call mpdatm3(xd1,xd2,xd3,xf,d,iflg)
!call mpdata3(xd1,xd2,xd3,xf,d,iflg)
endif
```

```
data mpfl,ampd/nth,0.00/
!data mpfl,ampd/ 6 ,0.00/
```

NH-IFS

ECMWF

Final comments

- **Herein some possibilities have been illustrated with time-dependent coordinate transformations in horizontal and vertical directions and its accuracy in wave-driven flows.**
- **Applications include two and three dimensions for laboratory scale, meso-scale and global-scale simulations in Cartesian, cylindrical or spherical geometry.**
- **There are many more interesting applications from moving sand dunes to stellar applications as illustrated in previous and forthcoming talks.**